DETECTING LEAFY SPURGE IN NATIVE GRASSLAND USING HYPERSPECTRAL IMAGE ANALYSIS

CATHERINE KLOPPENBURG

B.Sc., (Computer Science), University of Lethbridge, 2005

B.Sc., (Geography), University of Lethbridge, 2010

A Thesis
Submitted to the School of Graduate Studies
of the University of Lethbridge
in Partial Fulfillment of the
Requirements for the Degree

MASTER OF SCIENCE

Department of Geography
University of Lethbridge
LETHBRIDGE, ALBERTA, CANADA

DETECTING LEAFY SPURGE IN NATIVE GRASSLAND USING HYPERSPECTRAL IMAGE ANALYSIS

CATHERINE KLOPPENBURG

Approved:

* (Print Name)	(Signature)	(Rank)	(Highest Degree)	Date
Dr. Karl Staenz * Co-Supervisor	_____	_____	_____	_____
Dr. Anne Smith * Co-supervisor	_____	_____	_____	_____
Dr. Craig Coburn * Thesis Examination Committee Member	_____	_____	_____	_____
Dr. Nadia Rochdi * Thesis Examination Committee Member	_____	_____	_____	_____
Dr. Wei Xu * Chair, Thesis Examination Committee	_____	_____	_____	_____

ABSTRACT

Leafy spurge (*Euphoria esula* L.) is a perennial noxious weed that has been encroaches on the native grassland regions of North America resulting in biological and economic impacts. Leafy spurge growth is most prevalent along river banks and in pasture areas. Due to poor accessibility and the cost and labour associated with data collection, estimates of number and size of leafy spurge infestations is poor. Remote sensing has the ability to cover large areas, providing an alternate means to ground surveys and will allow for the capability to create an accurate baseline of infestations. Airborne hyperspectral data were collected over the two test sites selected on the Blood Reserve in Southern Alberta using a combined Airborne Imaging Spectrometer for different Applications (AISA) Eagle and Hawk sensor systems in July, 2010. This study used advanced analysis tools, including spectral mixture analysis, spectral angle mapper and mixture-tuned matched filter techniques to evaluate the ability to detect leafy spurge patches. The results show that patches of leafy spurge with flowering stem density >40 stems m^{-2} were identified with 85 % accuracy while identification of lower density stems were less accurate (10 - 40 %). The results are promising with respect to quantifying areas of significant leafy spurge infestation and targeting biological control and potential insect release sites.

ACKNOWLEDGEMENTS

I would like to thank my supervisors, Dr. Karl Staenz and Dr. Anne Smith, and my committee members, Drs. Craig Coburn and Nadia Rochdi, for their help and support throughout this process. I would like to thank Dr. Robert Bourchier for being able to answer all of my questions about leafy spurge, Dr. Jinkai Zhang for his help sorting out the many issues with my image data and reprocessing them for me, and Dr. Brian Van Hezewijk for his help with the stem density estimate process. I would like to thank Gary Larson and Ingrid Oseen for the advice, laughter, and encouragement they always seemed to have in abundance and always being there to listen to my rants whether they wanted to or not. I would like to thank Cale Fox, Leah Blair, Chaylene Little, Ashley Cutway, Ray Wilson, Monte Thomson, Lisa Zhang, Joe Buckley, and Steve Myshak for their help in collecting all of my field data.

The research for this project would not have been carried out without the funding from Agriculture and Agri-Food Canada, Natural Sciences and Engineering Research Council of Canada (NSERC), the Canadian Space Agency, and The University of Lethbridge as well as the Blood Tribe for granting access to their land for study purposes.

I would like to thank my family, friends, and all the important people in my life for their love and support throughout this time.

TABLE OF CONTENTS

LIST OF TABLES

LIST OF FIGURES

LIST OF ABBREVIATIONS

ADAR - Airborne Data Acquisition and Registration System
AISA - Airborne Imaging Spectrometer for different Applications
ALI - Advanced Land Imager
APDA - Atmospheric Pre-Corrected Differential Absorption
ASD - Analytical Spectral Device
ATCOR4 - Atmospheric Correction and Haze Reduction
AVIRIS - Airborne Visible/Infrared Imaging Spectrometer
DEM - Digital Elevation Model
DN - Digital Number
DSM - Digital Surface Model
EM - Electromagnetic
ETM+ - Enhanced Thematic Mapper
GPS - Global Positioning System
GSD - Ground Sampling Distance
HRV - High Resolution Visible
HSB - Hue, Saturation, Brightness
HyMap - Hyperspectral Mapper
IDW - Inverse Distance Weighting
IFOV - Instantaneous Field-of-View
ISODATA - Iterative Self-Organizing Data Analysis
LiDAR - Light Detection and Ranging
MESMA - Multiple Endmember Spectral Mixture Analysis
MF - Match Filter Score
MLC - Maximum Likelihood
MODTRAN - MODerate resolution atmospheric TRANsmission
MNF - Minimum Noise Fraction
MTMF - Mixture-Tuned Match Filtering
NDVI - Normalized Difference Vegetation Index
NIR - Near Infrared
PCA - Principal Component Analysis
RMSE - Root Mean Square Error
SAM - Spectral Angle Mapper
SMA - Spectral Mixture Analysis
SWIR – Short-Wave Infrared
SPOT - Système Pour l'Observation de la Terre
TM - Thematic Mapper
VNIR - Visible/Near Infrared

CHAPTER 1 INTRODUCTION

Native grasslands play a vital environmental role in water quality, soil conservation, wildlife habitat, and recreation (Marsett et al., 2006). The increasing demands on native grasslands have major impacts on climate change and the preservation of biodiversity with invasive species playing a large role in the ever changing global environment. Land-cover change is one of the detrimental environmental impacts mostly caused by industry, urban expansion, or agriculture (Turner II & Meyer, 1991). Previous research has shown that in some cases discrimination of an invasive versus a native plant species is possible using remote sensing due to their unique spectral signatures (Casady et al., 2005; Glenn et al., 2005; Parker Williams & Hunt, 2002 and 2004; O'Neill et al., 2000). The ability to separate an invasive weed at a variety of plant densities from other plant species and to show the presence of invasive plant species on native grasslands would prove to be useful for land managers (Masters & Sheley, 2001).

Remote sensing of native grassland has been used to help support the detection of the various forms of land-cover change and to monitor health, productivity, invasive species, and grazing pressure (Booth & Tueller, 2003; Tueller, 1989). Currently only 25 to 30 per cent (%) of the original grassland area remains in Canada, (Gauthier & Wiken, 2003). Approximately 25 million hectares of this area is in the western provinces and 10 million hectares are in Alberta (Figure 1-1). Within Alberta, 47.5 % of the native grasslands are located in the dry mixed sub-region (Adams et al., 2013).

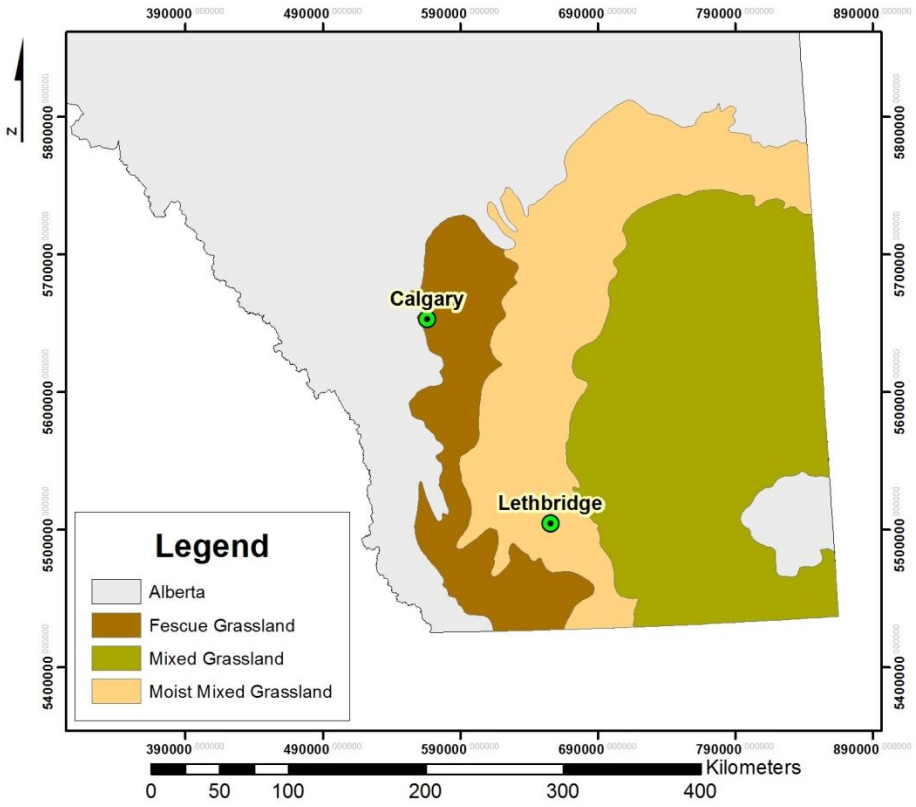

Figure 1-1: Ecozones of Alberta showing areas of native grassland.

Displacement of native grass species reduces flora and fauna biodiversity as well as the carrying capacity for the multi-billion dollar cattle industry which depends on native grasslands for forage (Everitt et al., 1995a). A 10-% reduction in cattle stocking rate as a result of the elimination, fragmentation or health degradation of the grassland would constitute a 12-million dollar loss (Luciuk et al., 1997). Despite the importance of grasslands, they are under threat due to expansion of cultivated agriculture, oil and gas exploration, invasive species, and urban development which are starting to limit the amount of grassland that is available for forage utilization (Parker Williams & Hunt, 2002; Smith & Buckley, 2011).

Leafy spurge (*Euphoria esula* L.) is a perennial, noxious, invasive weed that was first reported in North America in 1827 (Best et al., 1980). Leafy spurge is toxic to a number of livestock, including cattle (Best et al., 1980) as it acts as an irritant, emetic, and purgative that may result in livestock death. Currently, leafy spurge is a problem weed on more than 2 million hectares in 15 U. S. states and six Canadian provinces (Bell Randell & Lym, 2006), with the number of infestations doubling approximately every 10 years. Leafy spurge grows in a variety of landscapes, but it is most prevalent in areas along river banks, on pastures, and native grasslands, many of which are difficult to access (Bell Randell & Lym, 2006).

The encroachment of leafy spurge results in both biological and economic impacts including the potential to reduce carrying capacity of the land by 50 to 75 %. There is an estimated economic loss of 130 million dollars annually in North Dakota, South Dakota, Montana, and Wyoming (Hansen et al., 1997) and an estimated 16 million dollar economic impact in Manitoba (Leafy Spurge Stakeholders Group, 1999) due to the loss of grazing area through weed encroachment.

The ability to effectively map invasive weeds would assist in quantifying the loss of forage as well as enabling targeted control measures, such as the release of insects for biological control, targeted herbicides, and grazing sheep. Mapping will also allow the capability to quantify and validate the success or failure of these control methods. Creating an accurate baseline of infestations will provide an estimate of the biological and economic impacts of these weeds. Determining the extent of weed populations on native grasslands is difficult because of the great expanse and inaccessibility of these

areas (Everitt et al., 1995b). Studies in native grasslands of western Canada are absent due to the size of the area requiring monitoring and the associated cost and labour of data collection.

Remote sensing has proven to be a highly valuable tool for use in the fields of agriculture, geology, hydrology, oceanography, and environmental quality (Otterman et al., 1976; Purkis & Klemas, 2011). The detection of reflected or emitted surface electromagnetic (EM) energy is useful for obtaining information about certain types of ecosystems (Knipling, 1970). The reflected EM radiation is usually measured in the visible and near-infrared (VNIR) region (400-1000 nm) and shortwave infrared (SWIR) region (1000-2500 nm).

Remote sensing offers repeatable consistent data capture through the availability of satellite sensors and can provide more reliable information than ground-based sources (Defries & Townshend, 1999). With the ability of a single satellite image to cover large areas, applications of remote sensing would be less costly than ground mapping (Johannsen & Barney, 1981). Remote sensing provides coverage of large and inaccessible areas at a lower cost in terms of dollars and labour requirements.

Remote sensing of vegetation relies primarily on the detection of seasonal phenological signatures (Ustin & Gamon, 2010). Flowering leafy spurge shows distinct yellow-green bracts in the summer months and a red colouration of the stem in the fall as the plant starts to senesce (Figure 1-2). Previous studies showed the success in mapping leafy spurge is dependent upon exploiting the flowering of this species and the appearance of the yellow bracts in the summer (Casady et al., 2005; Glenn et al., 2005;

Parker Williams & Hunt, 2002 and 2004; O'Neill et al., 2000). As these reflectance characteristics are unique among the vegetation in the native grasslands, it will increase the success of using image data (Andrew & Ustin, 2008).

Figure 1-2: Photographs showing flowering leafing spurge stems (left) and senesced leafy spurge stems (right).

The goal of this research was to develop a baseline map showing the presence/absence and potentially density of leafy spurge for selected test sites. From the maps, vector layers were exported for use by end users of the technology, such as research scientists involved in biological control of leafy spurge and agricultural fieldmen responsible for inventory and control of leafy spurge.

The specific objectives pursued were to investigate the ability to separate leafy spurge at a variety of stem densities from native grasslands species and to develop a mapped product showing the presence or absence of leafy spurge on native grasslands using remote sensing technologies.

The main hypothesis tested in this thesis was that the leafy spurge spectral signature is separable from the spectral signatures of other species present in native grasslands during specific phenological stages.

CHAPTER 2 LITERATURE REVIEW

2.1 Introduction

The synoptic nature of remote sensing imagery coupled with advanced spectral capabilities afforded by hyperspectral imaging technologies and data processing techniques offer a powerful tool for mapping of invasive plant species. The management of invasive plant species is under represented in the remote sensing literature due to relatively small proportion of the landscape that these plants occupy. The increase in invasive plant species has threatened long-term ecosystem health and function as well as being potentially damaging to the livestock industry. This chapter presents a review of the diversity of research areas addressed by this thesis.

2.2 Impacts of Invasive Weeds

A number of different invasive weeds threaten native grasslands in North America (DiTomaso, 2000). Table 2-1 shows the top five most widespread invasive weeds in North America with each of them affecting more than 1 million hectares of grassland. The most common weeds in Southern Alberta are leafy spurge (*Euphorbia esula* L.), spotted knapweed (*Centaurea maculosa* Lam.), and Canada thistle (*Cirsium arvense* (L.) Scop.; Canadian Food Inspection Agency, 2008).

Table 2-1: Distribution of major grassland weeds (DiTomaso, 2000).

Species	Common name	Estimated infested area (Mha)
Centaurea maculosa Lam.	spotted knapweed	2.9
Centaurea diffusa Lam.	diffuse knapweed	1.3
Centaurea solstitialis L.	yellow starthistle	8.0
Bromus tectorum L.	downy brome	40.0
Euphorbia esula L.	leafy spurge	1.1

Research shows that it is necessary to establish a control program of some form in order to reduce the extent of invasive weed species and allow for the proper utilization of native grass for forage (DiTomaso, 2000; Hein & Miller, 1992). Leafy spurge has proven particularly difficult to control on untilled land because of its ability to spread rapidly, displace native vegetation, and sustain itself despite repeated chemical treatments (Hodur et al., 2006). Common methods of control include the release of insects for biological control, targeted herbicides, and multi-species grazing.

Leafy spurge propagates through not only the seed but also the root system making the elimination of the weed particularly challenging (Best et al., 1980). Many of these methods involve reducing the stalk of the plant leaving the root unaffected and, therefore, viable for regrowth. Thus, a combination of control methods usually provides the best results (DiTomaso, 2000; Best et al., 1980). Studies have found that it may take multiple years for the control to become visually evident. The annual cost of leafy spurge and spotted knapweed impact in Canada is considerable as shown in Table 2-2.

Table 2-2: Economic impact of invasive species in native grassland in Canada (Colautti et al., 2006). Characterized costs are in Canadian dollars per annum.

Name	**Impacted Area**	**Characterized Cost (x $1,000)**
Leafy spurge	Manitoba: reduced yield and recreation revenues, control costs	18,870
	Manitoba: reduced land value	30, 000*
	Alberta & Saskatchewan: reduced yield and recreation revenues, control costs	18,870
	Alberta & Saskatchewan: reduced land value	30,000*
Spotted knapweed	British Columbia: hay production	400
	British Columbia: grazing livestock	79

* Indicate one-time event

2.3 Remote Sensing Concepts

Remote sensing is defined as the collection of data by a sensor without physical contact with the study object (Jensen, 2005). Remote sensing systems have many different spatial, spectral, radiometric, and temporal resolutions. The spectral resolution of a sensor refers to the width of a band in an image characterized by the spectral response profile while the number of bands is defined by the spectral sampling (Figure 2-1). The spatial resolution of a sensor can be explained by the ground sampling distance (GSD) or the dimension in metres of the ground projected instantaneous field-of-view (IFOV). The former is the measure of the distance between the centers of two adjacent samples within the data collected by a sensor. A satellite sensor typically has a lower spatial resolution than an airborne sensor.

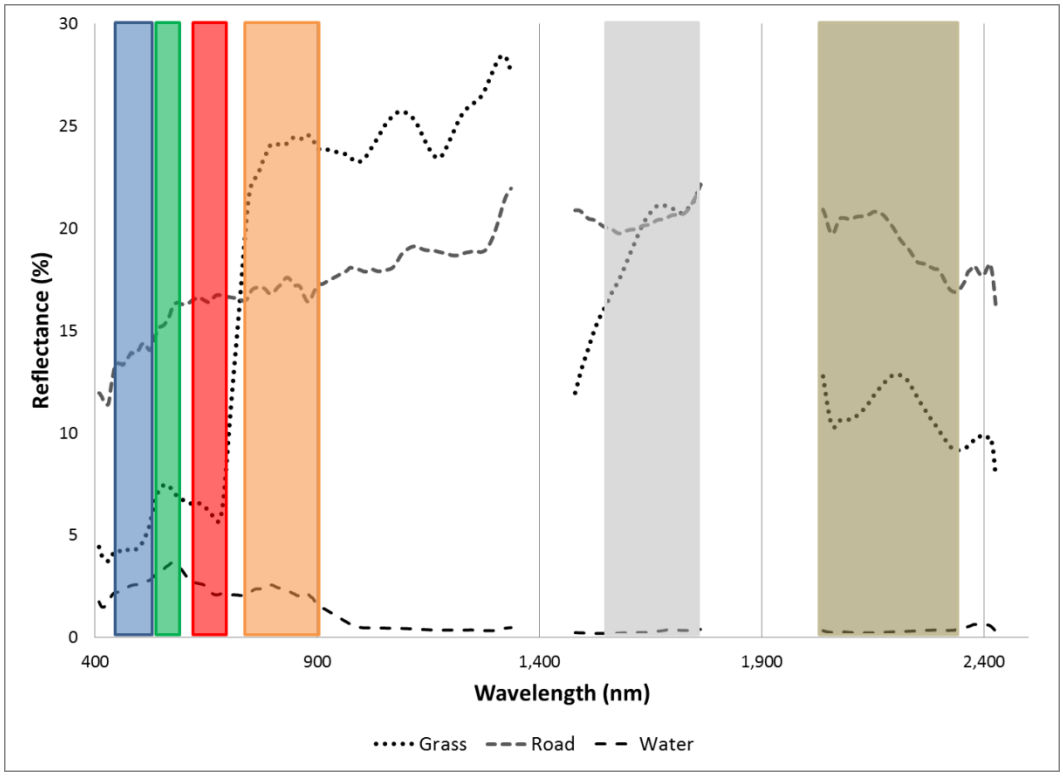

Figure 2-1: Comparison of multispectral versus hyperspectral spectral responses. The large coloured regions represent bands from Landsat TM (bands 1-5 and 7) and the spectra represent data found in a typical hyperspectral image.

Multispectral sensor systems, such as the Landsat Thematic Mapper (TM), Landsat Enhanced TM (ETM+), Système Pour l'Observation de la Terre High Resolution Visible (SPOT HRV), Advanced Land Imager (ALI), IKONOS, and Airborne Data Acquisition and Registration System (ADAR), use a small number of broad spectral bands to cover the wavelength regions (Mitchell & Glenn, 2009; Singh & Glenn, 2009; Hunt et al., 2007; Mladinich et al., 2006; Stitt et al., 2006; Casady et al., 2005; Carson et al., 1995). Hyperspectral imagers, such as the Airborne Visible/Infrared Imaging Spectrometer (AVIRIS) and Hyperspectral Mapper (HyMap) provide spectral data in ≥ 50 narrow contiguous bands each with a width of approximately 2 nm – 20 nm (Mitchell

& Glenn, 2009; Noujdina & Ustin, 2009; Hunt et al., 2007; Parker Williams & Hunt, 2004). Multispectral systems have been around since the mid-1960's and are more commonly used as it is costly to build hyperspectral satellite systems with the capabilities needed to solve finer resolution land-cover problems such as detecting small patches of invasive weeds. Hyperspectral systems are currently mostly mounted on airborne or ground platforms due to the large volume of spectral data collected with the image information.

2.4 Mapping of Invasive Weeds

Determining the impact of weed populations on native grasslands is difficult because of the large expanse and inaccessibility of these areas (Everitt et al., 1995a). Previous mapping attempts using remote sensing have relied primarily on the use of detecting the phenological (plant life stages) signatures of plants throughout the growing season (Ustin & Gamon, 2010). As an example, the success of mapping leafy spurge with remote sensing depends upon exploiting the appearance of yellow bracts during the flowering season (Casady et al., 2005; Glenn et al., 2005; Parker Williams & Hunt, 2002 and 2004; O'Neill et al., 2000). As these flowering characteristics are spectrally unique among the vegetation in the native grassland, they increase the ability to use remotely sensed data (Andrew & Ustin, 2008). Previous studies in the detection of invasive weeds, involving a variety of image classification methods provided differing degrees of success as shown in Table 2-3. The methods included both unsupervised and supervised classifications.

Table 2-3: Previous studies showing accuracies of different classifiers and image types for identifying invasive species.

Weed Type	Classifier	Image Data	GSD (m)	Accuracy (%)	Author
Downy brome	SMA[1]	Landsat ETM+	30	61 - 77	Singh and Glenn, 2009
Downy brome	MTMF[2]	AVIRIS	3 - 3.8	70 - 81	Noujdina and Ustin, 2009
Leafy spurge	MTMF	AVIRIS	20	75 - 97	Parker Williams and Hunt, 2004
Leafy spurge	MTMF	HyMap	3.2	67 - 85	Mitchell and Glenn, 2009
Leafy spurge	MTMF	Landsat TM	30	38 - 62	Mitchell and Glenn, 2009
Leafy spurge	MTMF	HyMap[6]	3.2	91-100	Mitchell and Glenn, 2009
Leafy spurge	ISODATA[3]	Landsat ETM+	15[7]	62 - 66	Mladinich et al., 2006
Leafy spurge	ISODATA	ALI	10[7]	66	Stitt et al., 2006
Leafy spurge	MLC[4]	IKONOS	4	56 - 87	Casady et al., 2005
Leafy spurge	SAM[5]	AVIRIS	20	56 - 74	Hunt et al., 2007
Leafy spurge	SAM	SPOT 4 HRV	20	48 - 61	Hunt et al., 2007
Leafy spurge	SAM	Landsat ETM+	30	49 - 59	Hunt et al., 2007
Yellow hawkweed	MLC	ADAR	1	81	Carson et al., 1995
Yellow hawkweed	unsupervised	ADAR	1	76	Carson et al., 1995

[1] Spectral Mixture Analysis (SMA)
[2] Mixture-Tuned Match Filter (MTMF)
[3] Iterative Self-Organizing Data Analysis (ISODATA)
[4] Maximum Likelihood (MLC)
[5] Spectral Angle Mapper (SAM)
[6] Spectral resolution was resampled to simulate Landsat ETM+.
[7] Native GSD of 30 m was resampled using the panchromatic band.

2.4.1 Unsupervised Classification

Unsupervised classifications, such as the Iterative Self-Organizing Data Analysis (ISODATA; Sabin, 1987), statistically clusters image data based on the spectral characteristics of individual pixels. Subsequently, the analyst can attribute cover types to the clusters.

Medium-resolution (~30 m GSD) multispectral images, such as acquired by Landsat 7 ETM+ (Mladinich et al., 2006) and ALI on board the Earth Observing-1 platform (Stitt et al., 2006), were classified using the ISODATA classifier in order to map areas of leafy spurge. The results showed that there were missing areas of known spurge accumulations along stream banks and an over estimation of spurge in areas such as cropped fields due to the spatial resolution and spectral domination in a pixel by a single feature.

Airborne ADAR image data were used to try to detect both yellow hawkweed (*Hieracium pretense* Tausch; Carson et al., 1995; Lass & Callihan, 1997) and yellow starthistle (Lass et al., 1996). A principal component analysis (PCA; Singh & Harrison, 1985) and an unsupervised classification were performed on the images in both studies. Carson et al. (1995) were able to detect yellow hawkweed with 76 % accuracy with some confusion with other grass-forb species in the area. Lass et al. (1996) found that the ADAR images provided adequate information on yellow starthistle to identify patches of 30 - 100 % ground cover for site-specific weed management. The ground coverage of the ADAR image data was a severe limitation in all studies as it can only cover 154 ha.

2.4.2 Maximum Likelihood Classification

Supervised classification has been used extensively with imagery for the identification and mapping of vegetation (Foody et al., 1992). This technique, which relies on the statistical properties of analyst selected training areas to train a classifier, differs from unsupervised approaches as the analyst is required to select representative areas of pixels and assign a class label prior to the classification stage.

Carson et al. (1995) used the maximum likelihood classifier (MLC) on 1-m ADAR images to try to determine populations of yellow hawkweed. Higher accuracies were found using the supervised classification (81 %) compared to the unsupervised classification (76 %). It was concluded that the major patterns of the weed in both types of classified images basically matched the observed image patterns that were in the study area.

Casady et al. (2005) used 4-m IKONOS multispectral data to determine if the use of spatially high-resolution multispectral data would achieve similar results to those found by Parker-Williams and Hunt (2002) but at a lower cost. In this case, MLC showed higher accuracies were achieved in areas of grassy land cover (87 %) as compared to dense shrubs and forbs (67 %). It is believed that many of the forbs in the one site were misclassified as leafy spurge.

2.4.3 Spectral Angle Mapper Classification

Spectral Angle Mapper (SAM; Kruse et al., 1993) uses the spectral similarity between image pixel spectra and reference spectra by calculating the angle between the vectors

defined by the reference spectrum and the spectrum to be classified (see Section 3.7.1). Smaller angles represent closer spectral matches.

Lass et al. (2002) used 5-m Probe-1 hyperspectral image data and SAM to detect spotted knapweed in Idaho with a validation site in Montana. Results showed that the use of wider angles in the classifier (14 - 20°) enabled identification of all areas of infestation, but tended to lead to confusion with some of the grasses in the landscape. The 11° angle was suitable for identifying spotted knapweed at densities of as little as 5 to 10 plants per pixel with 99 % accuracy. Subsequent testing of the derived method on a Montana verification site revealed identification of 18 out of 20 test sites selected.

Hyperspectral image analysis involving 20-m AVIRIS data and the SAM classifier proved effective for mapping leafy spurge areas with 93 % classification accuracy (O'Neill et al., 2000). Several classic multispectral transformations such as the normalized difference vegetation index (NDVI) and PCA were first used with the SAM approach. The resulting classified images from these methods did not match previous mapped patches or ground reference data; often drainage areas were misclassified as spurge. A Minimum Noise Fraction (MNF; Green et al., 1988) transformation was then applied to the same AVIRIS dataset to find the optimal bands to use with the SAM classifier. The result from the classified image using the MNF bands and SAM were the only ones to show patches of spurge infestation with patterns similar to a 1993 vector map of leafy spurge in the study area.

Hunt et al. (2007) investigated Landsat ETM+, SPOT 4 HRV, and AVIRIS datasets using the SAM classifier to identify leafy spurge patches. Different combinations

of visible and near-infrared bands and the full spectral range of the different image data were applied due to the distinct yellow-green colour of the leafy spurge bracts during the flowering season. The best results were found using the full spectral range of AVIRIS with 74 % accuracy. The low accuracies found with Landsat (49 %) and SPOT (48 %) data may be due to the coarser spectral resolution of these sensors.

2.4.4 Mixture-Tuned Matched Filtering

Mixture-Tuned Match Filtering (MTMF; Harsanyi et al., 1993) is a partial unmixing method that finds the abundance of a single endmember by maximizing the response of the known endmember and minimizing the response of the unknown endmembers (see Section 3.7.2).

Hyperspectral image analysis involving 20-m AVIRIS data acquired on July 6, 1999 in combination with MTMF proved effective for mapping leafy spurge areas with the presence/absence map having an accuracy of 95 % (Parker Williams & Hunt, 2002, 2004). The study areas that were misclassified tended to be in areas of woodland compared to grassland or the riparian cover types. The results suggest that MTMF could be used to establish an automated process for mapping leafy spurge.

Glenn et al. (2005) analyzed 3.5-m HyMap image data from 2002 and 2003 using MTMF to determine if high-resolution hyperspectral data could be used to repeatedly detect leafy spurge patches of differing densities over various years. Results showed that a minimum of 40 % leafy spurge ground cover was needed in order to obtain repeatable high accuracy results. With a ground cover of $\geq$ 40 % the classification accuracies were

93 % and 94 % for the respective years, while for less than 40 % ground cover the accuracies were 87 % and 86 %, respectively.

Mitchell and Glenn (2009) resampled the 121-band 3.2-m HyMap image data to simulate the spectral and spatial characteristics of the Landsat ETM+ and show how spatial and spectral resolution affect the ability to detect different leafy spurge density levels. The best results of the study (> 91 % accuracy) were obtained using the native 3.2-m spatial resolution of the HyMap data and the spectral resolution resampled to the six spectral bands of the Landsat ETM+ using the MTMF classifier. The results suggest it might not be necessary to use high-spectral resolution data to map leafy spurge (Table 2-3).

Downy brome was mapped by Noujdina and Ustin (2009) using 3.0 - 3.8 m AVIRIS data acquired in July 2000 and May 2003, respectively and the MTMF classifier. Image dates were selected based on specific stages in the downy brome life cycle and that of the surrounding native grasses and forbs. Downy brome was green in May and already senesced in July. Results showed that a multi-seasonal approach, using both the images from May 2003 and July 2000, was more accurate (81 %) in establishing a base map of downy brome infestation compared to the use of a single image collected in July 2000 (70 %). In July, downy brome tended to be confused with the forb tumble mustard (*Sisymbrium altissimum* L.) causing poorer accuracy results from the classification. However, the single-date image classifications in May tended to overestimate downy brome cover at lower-level densities (less than 40-% cover) and underestimate the downy brome cover at the higher-level densities (greater than 40 % cover).

2.4.5 Spectral Mixture Analysis

Spectral Mixture Analysis (SMA; Boardman, 1989) determines the abundance of a material by assuming that the pixel reflectance is representative of a combination of all pure target materials (endmembers).

Downy brome was mapped using a combination of four Landsat ETM+ images and SMA (Singh & Glenn, 2009). The study site had vegetation consisting of sagebrush and native grasses. Image data were acquired based on the peak greenness of the downy brome phenological cycle. The four images ranging in date from April 7 to June 26, 2002 were stacked to create a 24-band data cube and were then transformed using the MNF approach. Selected MNF bands were then used in the SMA. Endmembers were selected from areas within the scene using GPS coordinates collected from the known target areas. Two maps were created from this process: a percent ground-cover classification and a presence/absence map. Accuracies of 61 % and 77 %, respectively, were produced for these maps. Classification accuracies may have been influenced by the small number of validation points available. The study determined that different levels of downy brome cover should be tested in the future to determine the minimum plant density needed for detection.

2.5 Conclusion

Research shows that the use of remote sensing technologies can be effective in detecting the presence of invasive weeds in native grassland. Due to the complex nature of grassland-cover types, it might be more beneficial to use a partial unmixing method such as MTMF or a spectral matching method such as SAM instead of SMA due to the limitations in obtaining pure spectral signatures for all endmembers. The limiting factors in weed detection have been the coarse spectral and/or spatial resolution of the sensors (Table 2-3). In addition, a minimum plant density detection threshold needs to be determined in order to effectively establish robust procedures for repeatable detection of invasive species. Studies have shown that the use of higher spatial resolution in combination with higher spectral resolution image data improves upon weed detection and allows for higher mapping accuracies. Accordingly, this study will help establish a method for mapping leafy spurge using hyperspectral remote sensing technology.

CHAPTER 3 METHODS

3.1 Introduction

Remote sensing data collection and analysis have been used for the identification of various plant species using both multi – and hyperspectral methods. The identification of invasive weed species is particularly challenging due to the spectral and spatial similarity of weeds and native plant species. Using hyperspectral data and image classification techniques, this study developed a novel approach to the mapping of leafy spurge. This chapter describes the procedures used in this study to analyze and develop mapping techniques for detecting leafy spurge. The study area and the ground campaign are discussed followed by the stem density analysis, image processing steps, and validation of the maps retrieved.

3.2 Study Area

This study was undertaken at two different sites (Site 1: 49° 22' 3.83", -113° 4' 41.23"and Site 2: 49° 21' 56.13"; -113° 1' 24.07") on the Kainai (Blood Tribe) Reserve situated in the Foothills Fescue region of southern Alberta (Figure 3-1). Leafy spurge typically invades areas from the riparian zone to the adjacent grassland as the area around the river provides ideal growth conditions for the plant. The sites, which were located on floodplains in the St. Mary River, were surrounded by coulees. The soils in this region are predominantly in the Black Chernozem soil series (Alberta Agriculture and Rural Development, 2005). The climate of the region is characterized as cool continental and is defined by short hot summer months with ample precipitation and cold dry winters

(Natural Regions Committee, 2006). In July the mean temperature is 16.5°C with a rainfall average of 64.3 mm (Environment Canada, 2012). The study area was selected because there is a mix of grass, shrubs and forbs with adjacent cultivated crop fields and large patches of leafy spurge with differing stem densities.

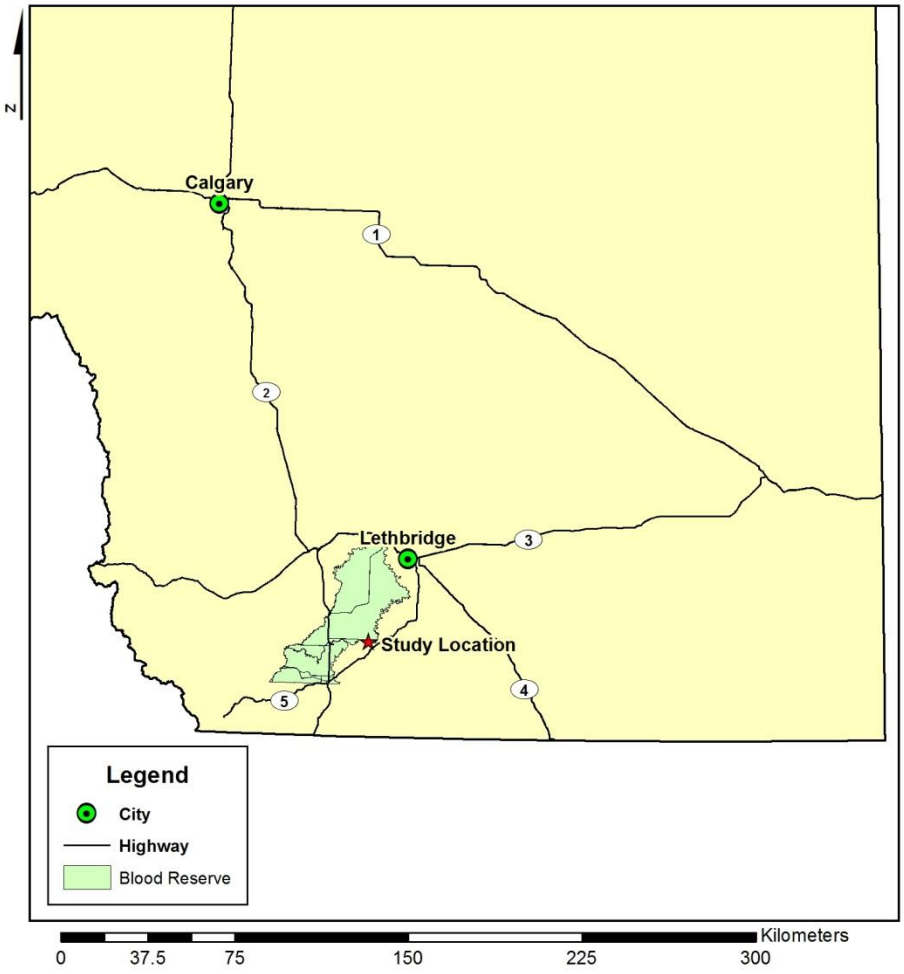

Figure 3-1: Map of Alberta showing the location of the area selected for study (top) with ground photographs showing differing leafy spurge densities at site 1 (left) and site 2 (right).

3.3 Image Acquisition

Airborne hyperspectral images were collected over the test sites using a combined Airborne Imaging Spectrometer for different Applications (AISA) Eagle and Hawk sensor systems (http://www.specim.fi; Figure 3-2). The AISA hyperspectral sensor system provided 492 bands of data in the VNIR and SWIR wavelength regions covering a wavelength range from 400 to 2500 nm. The spectral resolution was 2.4 nm in the VNIR range and 6.3 nm in the SWIR range. The data were collected at a 2-m GSD along with coincident Light Detection and Ranging (LiDAR) data and 25-cm true colour aerial photographs acquired from the same imaging platform. The LiDAR data were processed by the University of Victoria to obtain a digital surface model (DSM) as well as a bare Earth digital elevation model (DEM; Figure 3-3). The horizontal accuracy of the DSM and DEM were within 25 cm when checked relative to collected ground control-points. The image acquisition coincided with flowering of the leafy spurge on July 18, 2010 (Table 3-1).

Table 3-1: Sensor specifications.

Sensor	**No. of bands**	**Spectral resolution (nm)**	**Spectral coverage (nm)**	**Spatial resolution (m)**
AISA	492	2.4 (VNIR) 6.3 (SWIR)	400 - 2500	2
LiDAR	1	2 – 4 points per m^2	1060	0.2
DSLR Nikon D3	3	-	Visible	0.25

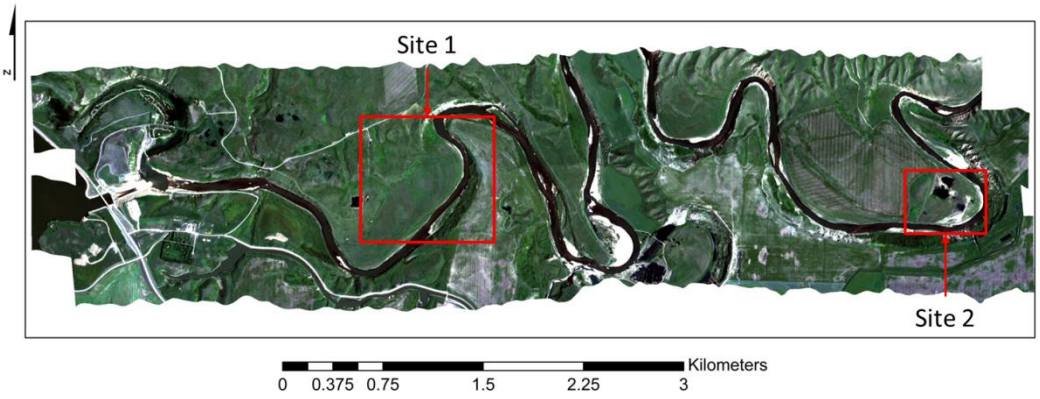

Figure 3-2: Study areas in the flats of the St Mary River in southern Alberta showing a true-colour composite AISA image in blue: band 24 (459 nm), green: band 64 (548 nm), and red: band 103 (638 nm).

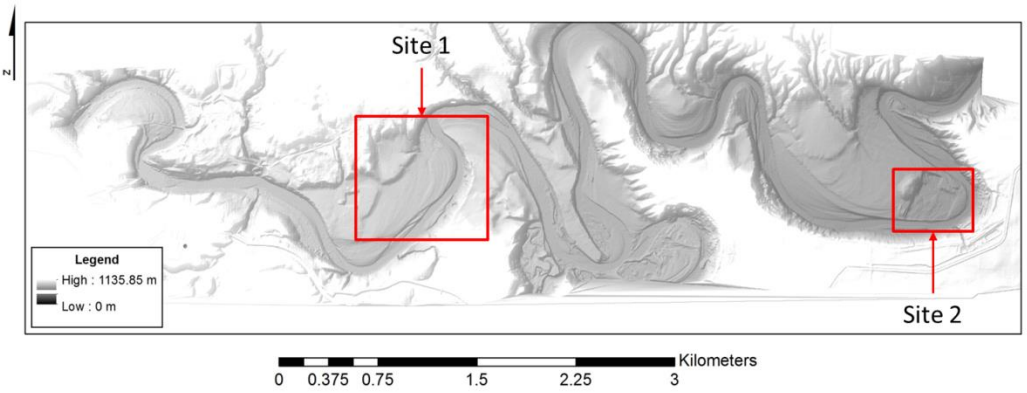

Figure 3-3: DEM of study site derived from LiDAR data showing relative height.

3.4 Ground-Data Collection

Extensive biophysical ground-data collection was completed within 3 days of the AISA image acquisition. Stem density estimates were collected in the field on July 20 and 21, 2010 to help with the validation of the interpreted image data collection and to

establish a pattern with respect to the stem density of the patches. Due to weather conditions, ground spectra were not collected until August 4 and 5, 2010. These data were used to determine if there was the potential ability to separate the different elements of the grassland scene based on spectral characteristics.

3.4.1 Stem Density Estimates

At each site, 100 m x 100-m plots, three at site 1 and one at site 2, were established encompassing differing levels of leafy spurge infestation (Figure 3-4). Within the plots, a grid sampling scheme of every 5 m x 5 m at site 1 and every 10 m x 10 m at site 2 was established (Figure 3-5). Site 2 was primarily used for validation of the classification process, and it was determined that the intense 5 m x 5 m grid sampling method was not required. The plots were geolocated using a Garmin Oregon 550 GPS (Garmin, Kansas) and a SX Blue sub-meter GPS (http://sxbluegps.com/product/sxblue-gps) with approximately 400 samples per sampling plot. Three digital photographs were taken at 0°, 90°, and 270° azimuth at each grid point relative to the direction of the transect from 2 m above the ground using the camera on the GPS unit (Figure 3-5). Manual stem counts were also conducted in three of the transects in each grid. At each of these latter grid points leafy spurge stems (both flowering and vegetative) were counted in a 0.25 m^2 frame (Figure 3-6) to provide a quantitative estimate of stem density. The frame size was chosen as it was large enough to capture a subset of the surrounding patch density while still fitting inside the 2-m pixel size of the airborne imagery.

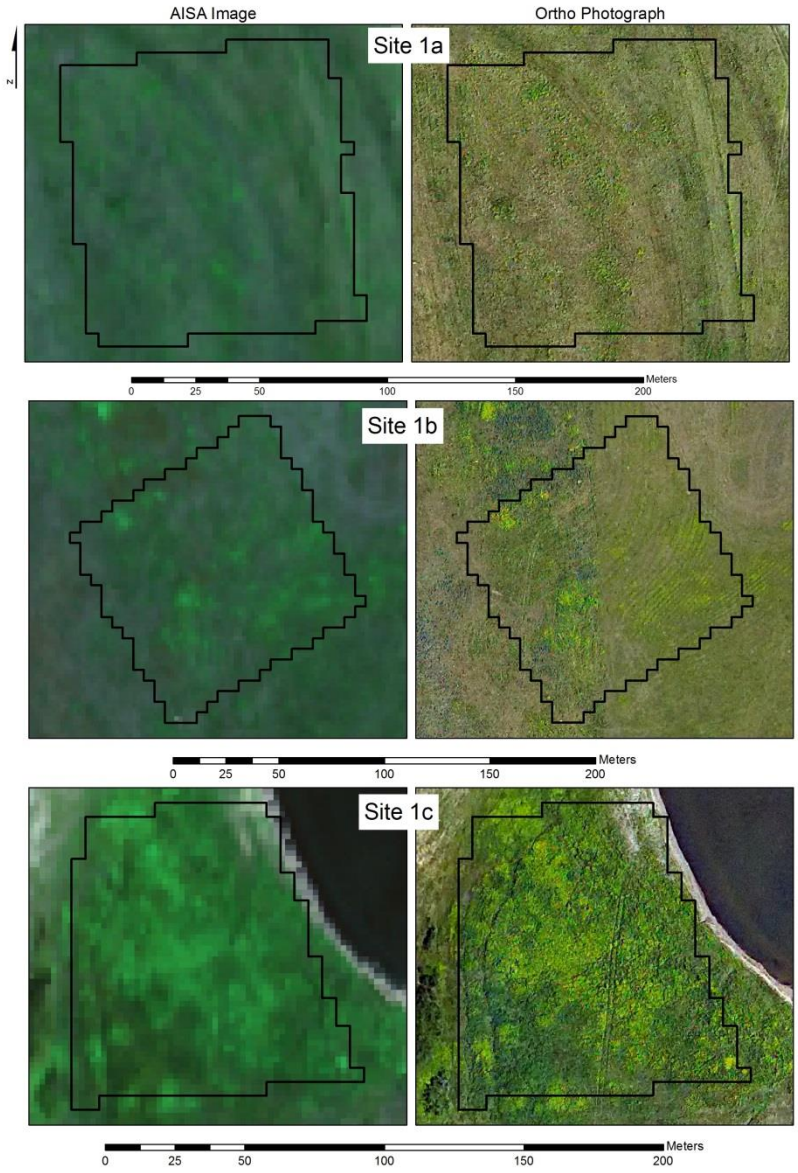

Figure 3-4: Spatial subsets of the AISA images (left) and ortho photographs (right) over Site 1. Black boxes show the location of the 100 m x 100 m sampling plots at each of the site.

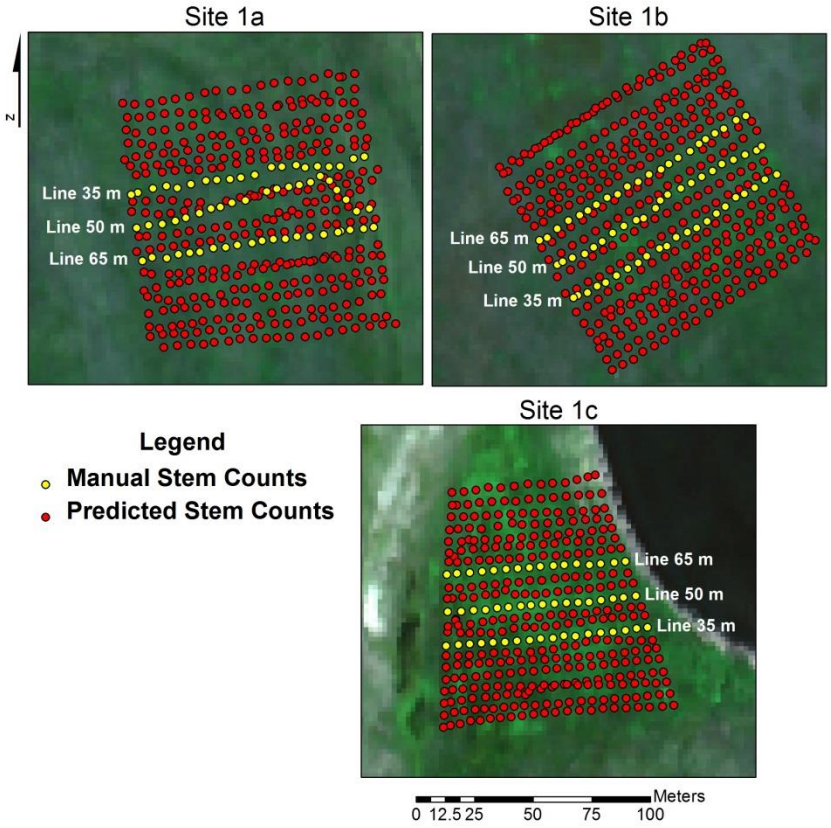

Figure 3-5: Sample plots at Site 1. Red points indicate areas where photographs were collected. Yellow points indicate areas where manual stem counts in addition to photographs were collected.

Figure 3-6: Frame used to collect stem density count data.

3.4.2 Ground-Spectra Collection

Ground spectra were collected at both sites 1 and 2 using an Analytical Spectral Device (ASD) FieldSpec 3 Portable Spectroradiometer with a spectral range from 350 nm to 2500 nm (ASD, 2007). The spectral resolution for the ASD is 3 nm in the VNIR and 10 nm in the SWIR with a sampling interval of 1.4 nm within the 350 to 1000 nm range and 2 nm in the 1000 to 2500 nm-range. The ASD was fitted with an 8° foreoptic and all measurements were taken at nadir at a height of 50 cm above the canopy resulting in a ~7 cm diameter IFOV.

ASD spectra were collected between 10:30 and 14:00 MST with no collection during periods of cloud cover. The ASD measurements were calibrated and corrected to reflectance with the program RS^3 (ASD, Boulder, Colorado) using a Spectralon™ panel at nadir every 15 minutes or after periods of cloud cover. The formula used to calculate the reflectance is as follows:

$$\text{Reflectance}_{(\theta s,\theta v)} = \frac{\text{target radiance}}{\text{panel radiance}} \times \text{Refcal}\,, \qquad (3.1)$$

where θ_s is the solar zenith angle, θ_v is the viewing angle and Refcal is the actual panel reflectance for a given wavelength. The spectral reflectance for a given θ_s and at nadir viewing angle is then computed over the full wavelength range at the given spectral resolution (Peddle et al., 2001).

A minimum of 10 spectral sample points of each ground-cover type, which included grass, bare soil, and leafy spurge, were collected *in situ* at both test sites. A total of 10 spectral radiance readings at each sample point were collected, and the reflectance was

computed using the panel and then averaged. The geographic coordinates of the sampling points were collected with the sub-meter SX Blue GPS, and photographs were taken using the camera on the Garmin Oregon GPS (Figure 3-7).

Figure 3-7: Sample photograph of grass (left), leafy spurge (middle), and bare ground (right) taken at the sites of ground spectra collection.

3.5 Stem-Density Photograph Analysis

The digital photographs collected with the Garmin Oregon GPS unit were analyzed using an image classification scheme to identify yellow pixels associated with flowering leafy spurge. They were processed to derive an estimate of the number of stems in high (> 40 stems m^{-2}), medium (15 - 40 stems m^{-2}), and low (1 -14 stems m^{-2}) density leafy spurge patches. Figure 3-8 shows the workflow of the full analysis for extracting the flowering leafy spurge stem counts from the photographs.

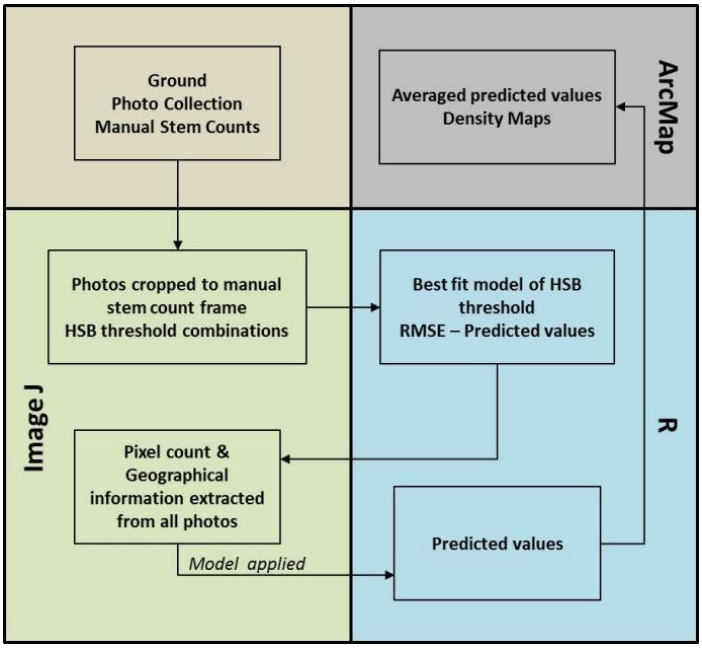

Figure 3-8: Flow chart showing the processing workflow of ground data related to flowering leafy spurge density estimates using the ground photographs. The root mean square error (RMSE) and hue, saturation, brightness (HSB) were used in this method.

Two different software packages were used for this process. ImageJ, a public domain Java-based image processing program, was used to edit and classify the photographs. R, a free software package for statistical computing (Bell Laboratories) was used to calculate statistics and stem densities based on the outputs from ImageJ. ESRI ArcMap 9.3 was used to create stem density maps using the combined results from ImageJ and R.

Photographs for which manual stem counts were also available (~200) were cropped in ImageJ to the area encompassing the 0.25 m^2 sample frame. A hue, saturation, brightness (HSB) colour threshold procedure was applied to extract the pixels that were in the yellow-green visible range in each of the photographs using the digital number

(DN) values of 0 - 255 in each photograph (Figure 3-9). All possible combinations of hue, saturation and brightness values were tested using increments of 5 DN in hue to encompass the range of the yellow and green pixels and increments of 51 DN in saturation and brightness were selected to create 5 equal range intervals. The procedure was based on previous work conducted in 2009 by B. Van Hezewijk (personal communication, December 1, 2010). A total of 311,850 combinations were tested in R to determine the optimal combination of parameters for identifying flowering leafy spurge from the photographs.

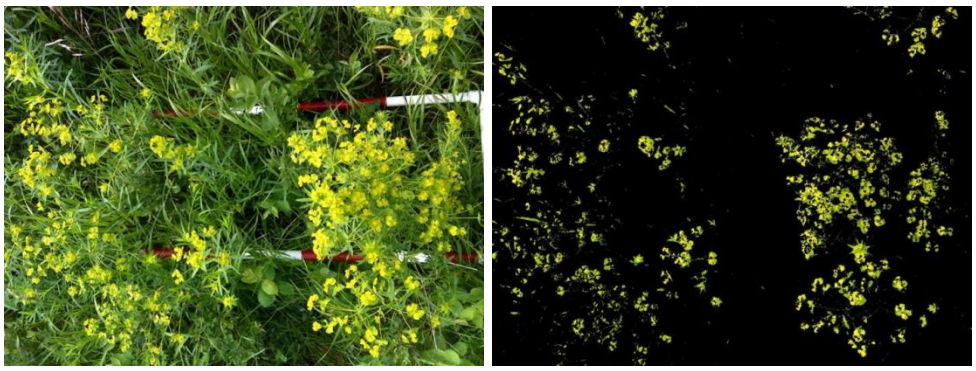

Figure 3-9: Before (right) and after (right) photographs showing the remaining green-yellow areas of the leafy spurge stem after the colour threshold procedure was applied.

Using the optimal combination of parameters, the relationship between the actual flowering stem counts and the yellow-green pixel counts was established in R using half of the photographs for which coincident manual stem counts were available, while the other half of the photographs were used to validate the relationship (Figure 3-10). The

relationship chosen was based on the lowest root mean square error (RMSE) of predicted flowering versus actual (observed) flowering stems. The RMSE is defined as follows:

$$\mathrm{RMSE} = \sqrt{\frac{1}{n}\sum_{i=0}^{n}\left(P_i - \hat{P_i}\right)^2}\ , \qquad (3.2)$$

where n is the number of observations, $\hat{P_i}$ is the predicted value at locations i and P_i is the actual value.

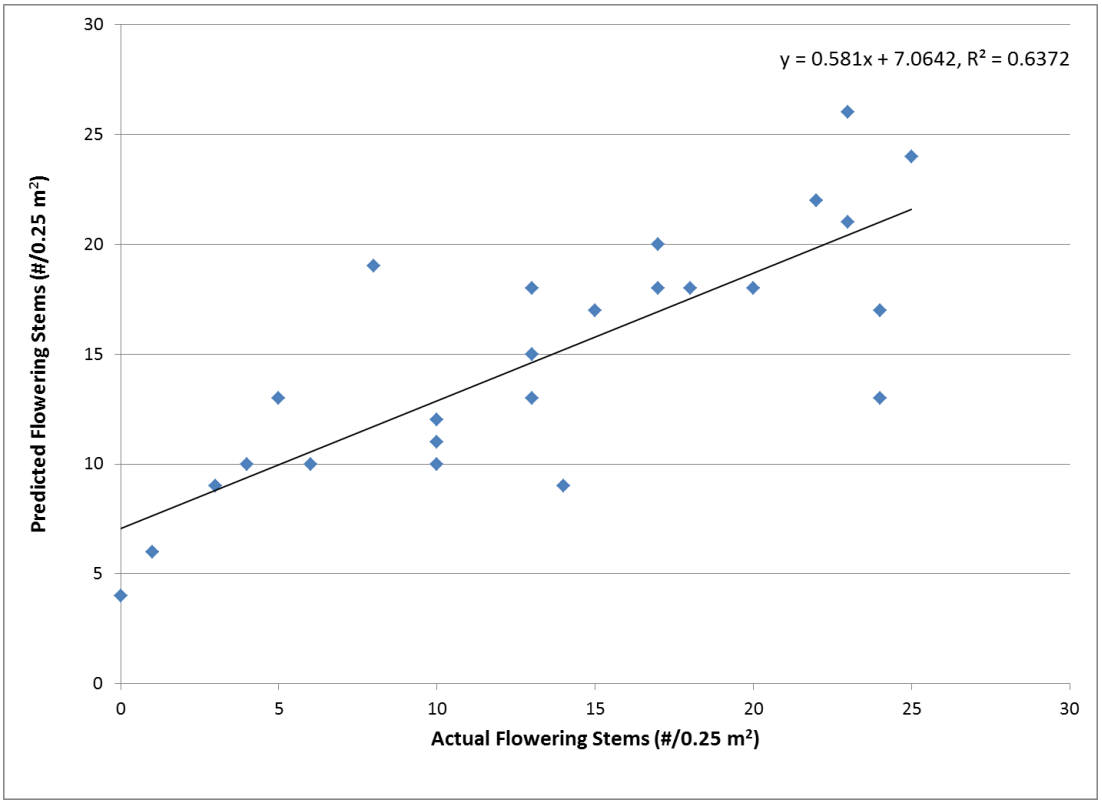

Figure 3-10: Actual flowering stem values compared to predicted flowering stem values for the validation data at Site 1c. Values were used to establish a relationship between stem counts and yellow pixels in ground photographs.

The relationship developed was used to extract leafy spurge flowering stem density estimates from all photographs for which geographic coordinates were available. Predicted leafy spurge flowering stem counts were averaged for the three photographs collected at each sampling point to provide an estimate for the 5 m^2 area around the sampling point.

Leafy spurge stem density maps were created in ESRI ArcMap 9.3 using an inverse distance weighting (IDW) algorithm as follows:

$$Z(s_0) = \sum_{i=1}^{n} W_i \, Z(s_i) \ , \qquad (3.3)$$

where $Z(s_0)$ is the value at unknown locations and is determined by the weighting value (W_i) and $Z(s_i)$is the value at known locations. This method was selected because it assumes the influence of the sample decreases with distance from the target and assigns a weighting accordingly (Lu & Wong, 2008). Roberts et al. (2004) used IDW to successfully map invasive weeds.

3.6 Image Analysis

Two flightlines containing the study areas were processed for use in the analysis. The software package ENVI/IDL was used for the image classification process (Exelis, 2009). Figure 3-11 summarizes the analysis work flow.

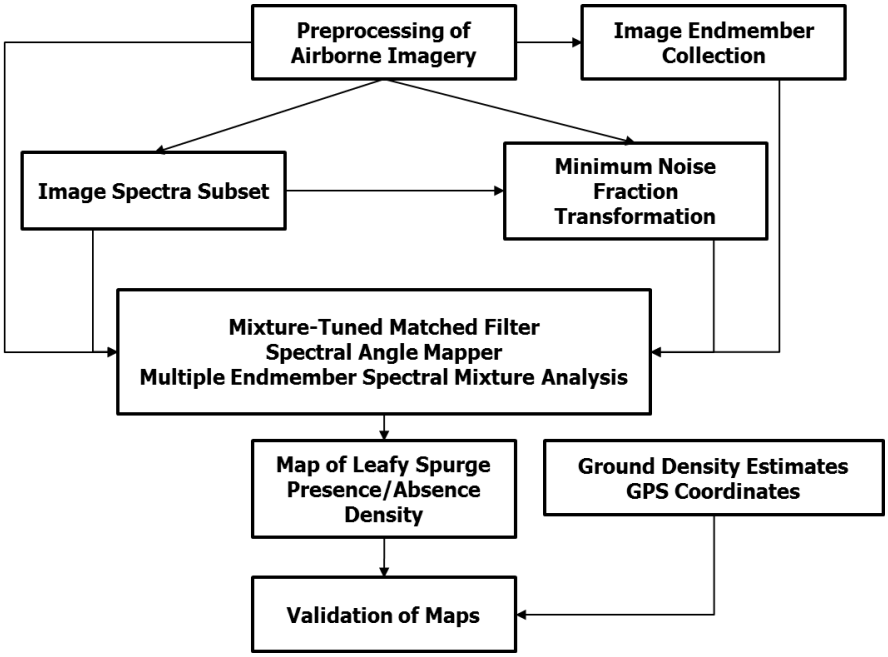

Figure 3-11: Outline of the image analysis work flow.

3.6.1 Image Preprocessing

Preprocessing of the AISA data included radiometric, atmospheric and geometric corrections. The transformation from raw data to radiance was done using an ENVI/IDL procedure that was developed by the University of Victoria specifically for AISA. It uses the imagery together with dark and calibration files to perform the transformation (Goodenough et al., 2009).

Due to an unsatisfactory atmospheric correction by the data providers, the step was conducted at the Alberta Terrestrial Imaging Center of the University of Lethbridge using ATCOR4, which is based on MODTRAN 5 (Richter & Schlapfer, 2002). Within this step, the at-sensor radiance is converted to surface reflectance. The water vapour was

estimated using the 940-nm absorption region and the atmospheric pre-corrected differential absorption (APDA) technique (Schläpfer et al., 1998). The values within the oxygen absorption region at 760 nm and the water vapour absorption regions at 820 nm, 940 nm and 1130 nm were linearly interpolated to reduce noise. A seven-band smoothing window was applied to spectrally smooth and reduce random noise and artifacts in the image spectra. The strong water absorption bands centered at 1350 nm and 1870 nm were removed leaving 419 bands for data for processing.

The geometric correction was performed using a program developed by the Department of Geography at University of Victoria in conjunction with Terra Remote Sensing Inc. (Sidney, BC, Canada). The navigation files along with LiDAR data and a DEM/DSM derived from the LiDAR data were used in a proprietary method to carry out the rectification (Goodenough et al., 2008).

The purpose of this study was to determine if varying leafy spurge stem density levels are detectable using hyperspectral images. All non-vegetated areas such as the St. Mary Dam, St. Mary River, and buildings were removed from the analysis. The normalized difference vegetation index (NDVI; Richardson & Wiegand, 1977) and threshold levels were used to identify and build a mask of these features (Figure 3-12). The NDVI was chosen as it is a simple and standard method of identifying vegetation in an image. This index is computed as

$$\mathrm{NDVI} = \left(\frac{\mathrm{NIR}-\mathrm{RED}}{\mathrm{NIR}+\mathrm{RED}}\right), \tag{3.4}$$

where NIR is the reflectance in the AISA band centred at wavelength 800 nm and RED is the reflectance at 670 nm (Haboudane et al., 2004).

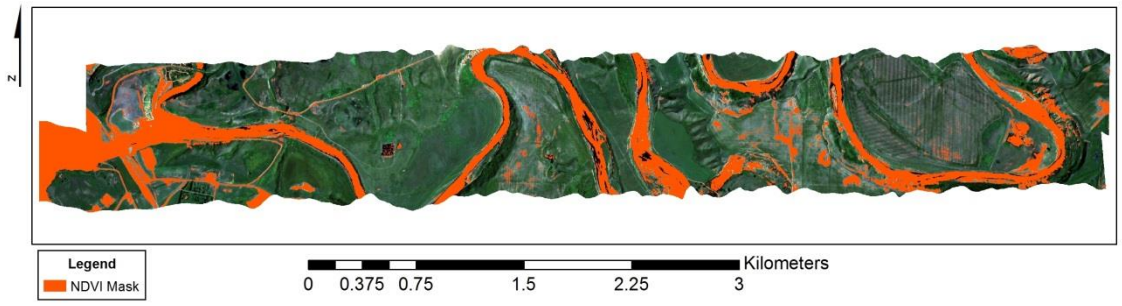

Figure 3-12: Orange areas indicate the derived NDVI mask to remove non-vegetated areas from the image.

3.6.2 Image Endmember Collection

The spectral signatures of flowering leafy spurge and associated grassland vegetation were located in the imagery using the ground data collected with the GPS units and the aerial photographs. All spectra were visually examined using the ENVI spectral plot function to evaluate spectral separability. Spectra manually collected from the image data based on identified ground locations from the field campaign showed the separability amongst different vegetation types (Figure 3-13). Pixels in areas with the most dense patches of leafy spurge were selected for use as an endmember with the classification algorithms.

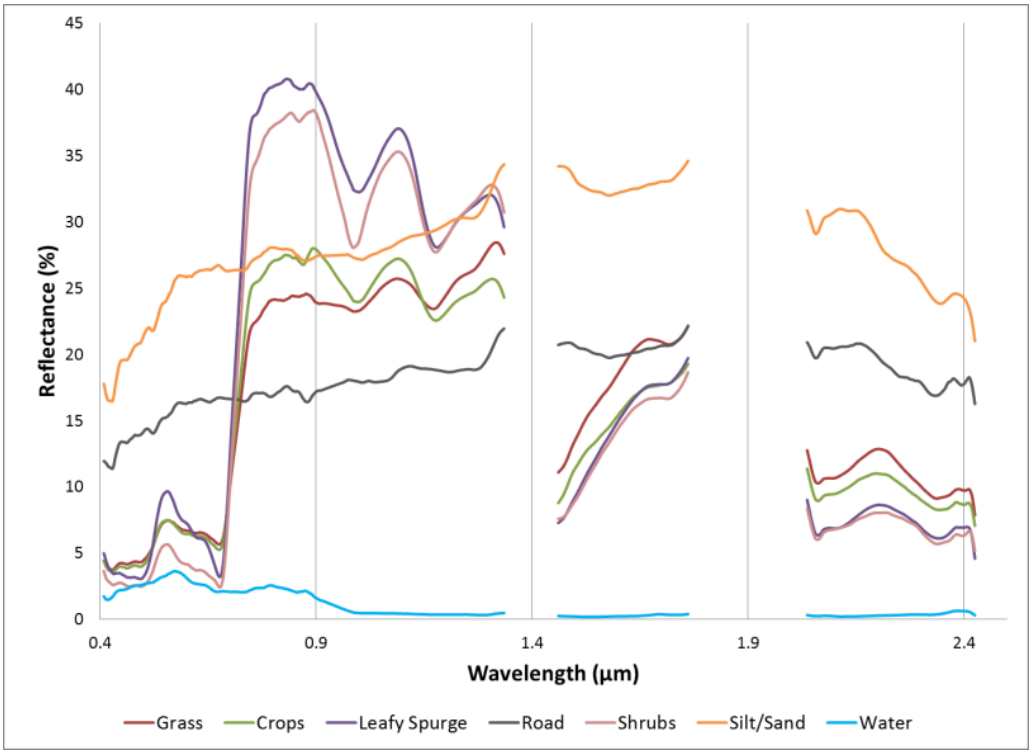

Figure 3-13: Sample of image (endmember) spectra showing visible separability. For example, water is distinct from other terrestrial targets while the vegetation types show a similar spectral curve in the NIR and SWIR wavelength ranges.

3.6.3 Image Spectra Subset

A variety of image band subsets were selected in addition to the full wavelength band set to determine if a reduced wavelength range could be used in identifying flowering leafy spurge similar to the process used in Hunt et al. (2007). Two reflectance subsets (450-794 nm and 495-668 nm) were generated based on the visual separability of the different image endmembers selected from the image.

3.6.4 Minimum Noise Fraction Transformation

The MNF is a linear transformation that uses two separate principal component analysis rotations as a way to decorrelate and rescale noisy data (Lee et al., 1990; Green et al., 1988). It is a method which can be used to reduce the number of spectral bands that are input into a classifier. This transform was applied to the entire band set and also the various subsets. The bands used in the classification process were selected from each flightline by determining the brightness differences and the visibility of landform characteristics in each MNF band. Different band numbers were selected based on the flight line and the band subset used. Figure 3-14 shows a sample of the resulting bands from a MNF transform with varying degrees of usefulness as determined by visual examination.

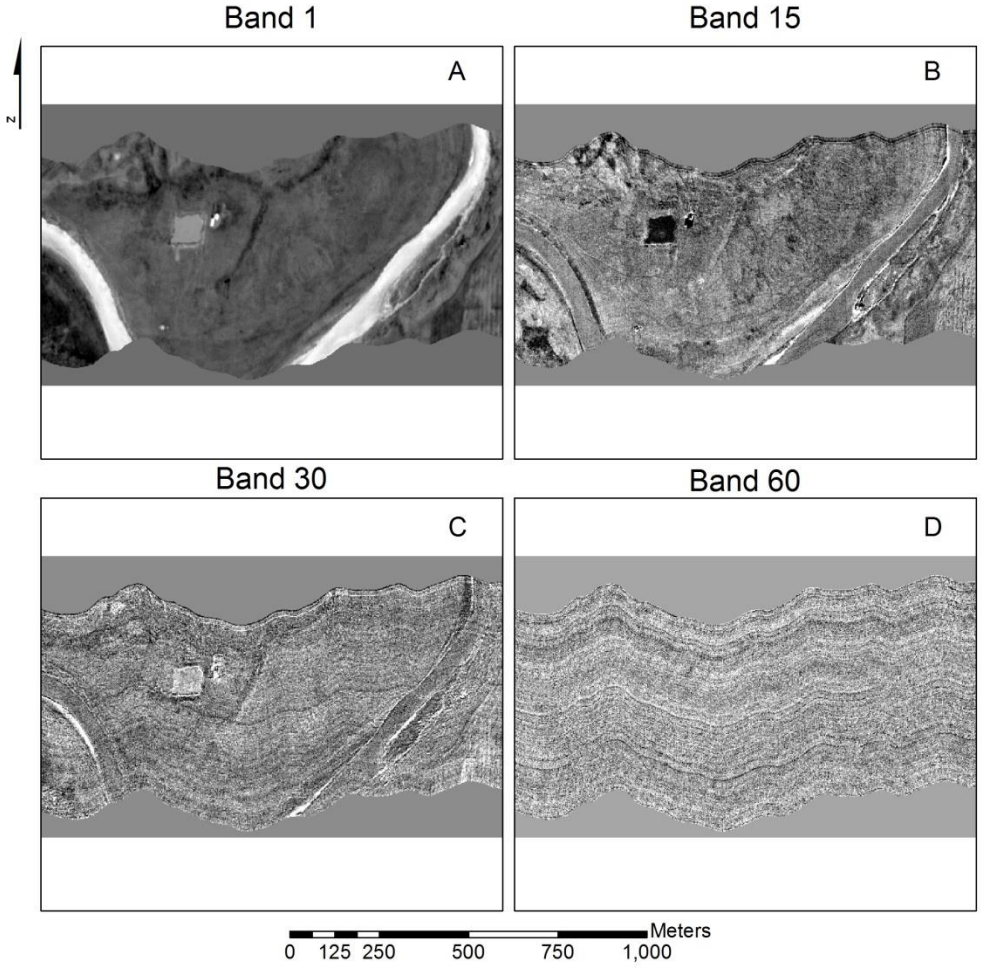

Figure 3-14: Sample of four bands (Band 1, Band 15, Band 30, Band 60) from the MNF transform applied to the full spectral range of AISA data.

3.7 Image Classification

Previous research studies show that the use of remote sensing can be effective in detecting the presence of leafy spurge in native grassland. A variety of classification algorithms as described in chapter 2, including MTMF (Mitchell & Glenn, 2009; Andrew & Ustin, 2008; Glenn et al., 2005; Parker Williams & Hunt, 2004), SAM (O'Neill et al.,

2000), and SMA (Elmore et al., 2000) were tested using the reflectance data and the MNF transformations from the complete and the two subset image datasets to map the presence or absence of flowering leafy spurge.

3.7.1 Spectral Angle Mapper

Six different images from both flight lines were used for the SAM classifier. Three images using the different selected image band sets in reflectance and three band sets transformed into MNF were input into the SAM classification to derive the best results. Classification angle values were derived in radians using the following expression (Kruse et al., 1993):

$$\alpha = \cos^{-1}\left(\frac{\sum_{i=1}^{nb} t_i r_i}{\left(\sum_{i=1}^{nb} t_i{}^2\right)^{1/2}\left(\sum_{i=1}^{nb} r_i{}^2\right)^{1/2}}\right), \qquad (3.5)$$

where t is the test spectrum, nb is the number of bands, and r is the reference spectrum (Figure 3-15). The latter was chosen based on the amount of leafy spurge that was present in the classification preview. A single threshold value was selected for all classes in the whole image with pixels being classified that had an angle value close to 0°.

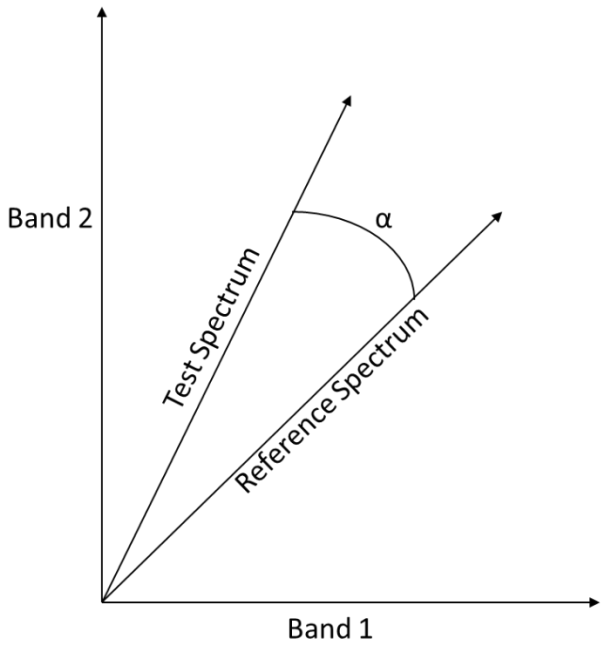

Figure 3-15: Plot of a reference spectrum and test spectrum for a two-band image. The same materials with varying illumination are represented by the vectors connecting the origin (no illumination) and projected through the points representing the actual spectra.

3.7.2 Mixture-Tuned Matched Filtering

The three image band sets were transformed using the MNF and then classified using the MTMF method. The MTMF process resulted in a set of two images that show the Matched Filter (MF) score and the infeasibility number (Figure 3-16; Boardman & Kruse, 2011). Areas of the image are then selected using a high MF score and a low infeasibility score where the closer the MF score is to 1.0 the better the match is between the endmember and the spectral sample. The infeasibility score is used to reduce the number of false positives present in the classified results.

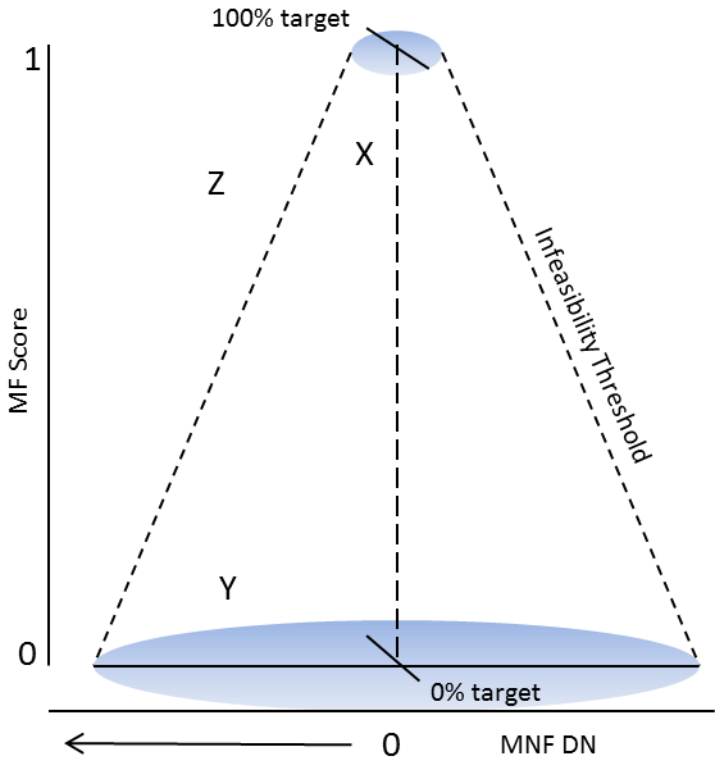

Figure 3-16: Diagram illustrating the MTMF concept where X is a match due to a high MF score, Y is excluded due to a low MF score, and Z is excluded due to a false positive match.

3.7.3 Multiple Endmember Spectral Mixture Analysis

Multiple Endmember Spectral Mixture Analysis (MESMA) was used due to the inability to obtain all of the endmembers present in the image scenes. MESMA allows a combination of different endmembers to model the linear sum of spectra on a per-pixel basis. It requires a model to meet minimum fit, fraction and residual constraints while using every combination of two, three, and four endmember models to unmix the image (Powell et al., 2007). Multiple image endmembers were selected for leafy spurge as well as grass and other vegetation present in the scene (Figure 3-13).

3.8 Validation

The classification methods were validated using a log-linear analysis model (McCloud & Darroch, 1995) based on the comparison of the number of pixels classified in a specific density class and the total number of pixels found in that class (Table 3-2). The initial stem density data collected in the field were used for this process (Figure 3-4).

Table 3-2: Classification inputs for log-linear analysis.

Density	Stem density per m^{-2}	Classifier	Classification Pixel Count	Density Pixel Total
Low	1-14	SAM	42	778
Medium	15-40		81	269
High	>40		138	173
Low	1-14	MTMF	47	778
Medium	15-40		105	269
High	>40		154	173
Low	1-14	SMA	71	778
Medium	15-40		118	269
High	>40		143	173

Follow-up field campaigns were conducted in October 2011 and July 2012 to collect GPS points/polygons and stem density estimates to validate the image classification results. Areas of pixels classified in the imagery as leafy spurge were located on the ground in the fall of 2012 using a GPS to determine if there was or there had been leafy spurge present. Areas of non-leafy spurge in the classified images were also investigated. A more thorough field campaign was carried out in the summer of 2012 when the leafy spurge was flowering as it was easier to detect the patches when

leafy spurge was yellow than during the fall when it was red. Six sites were selected but due to the limited access to the validation sites, random transects were paced every 10 m through only two areas identified as leafy spurge in the classified images. Leafy spurge stem density, both flowering and vegetative stems were counted using the 0.25 m^2 frame that was utelized in the initial field campaign. The transects started before and ended after the boundary of the identified patches to encompass a variety of all different densities of the spurge including no leafy spurge (Figure 3-17).

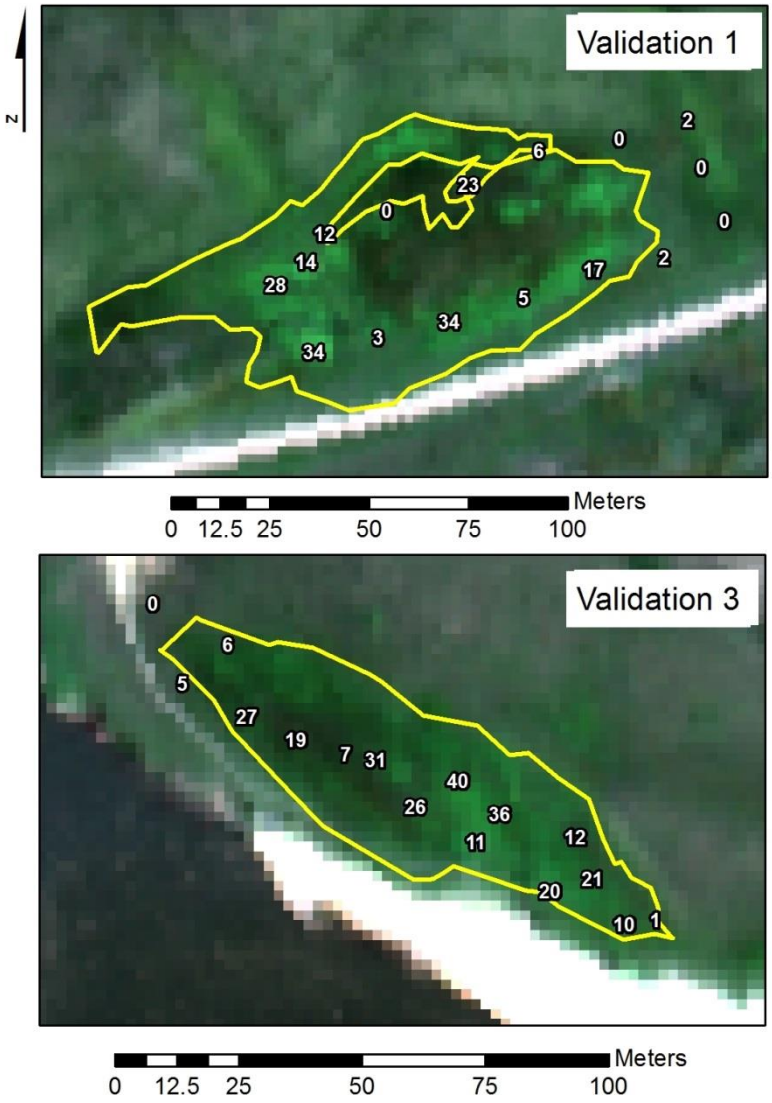

Figure 3-17: Validations sites 1 (top) & 3 (bottom) showing additional stem density counts from July 2012 overlaid on a true-colour composite AISA image (blue: band 24 (459 nm), green: band 64 (548 nm), and red: band 103 (638 nm)).The yellow line indicates a polygon walked with a GPS.

CHAPTER 4 RESULTS AND DISCUSSIONS

4.1 Introduction

The purpose of this research was to investigate the utility of hyperspectral remote sensing techniques to discriminate between leafy spurge and native grasslands. Airborne AISA data were collected and processed to establish a method for determining the presence of leafy spurge in native grassland. Field data comprised of stem density counts, photographs and ground spectra were collected to compare the leafy spurge stem density that was found on the ground to the density that could be detected in the image data. The stem density estimates also showed where relatively pure endmembers could be collected in the image for use in the classification methods.

The SAM, MTMF and MESMA algorithms were tested using all wavelengths as well as various band subsets composed of different spectral wavelengths. The results show potential for patch detection and a presence/absence map of leafy spurge locations over a larger area was created using these image classifiers. Validation data were also collected in the field, which were used in combination with the stem density estimates to determine the accuracy of the derived maps.

4.2 Data Preprocessing

Results from the final processing of the image data are shown in Figure 4-1 for the two flightlines. They indicate that the reflectance in the SWIR regions around 1300-nm, 1800-nm, and 2050-nm are too high. In addition, there were areas in the spectra after 660 nm (in between the chlorophyll well and the near-infrared plateau)where the spectral curves appeared to have been interpolated and were represented as a straight line. Several attempts were made to correct the issue and produce a spectral curve for the image elements.

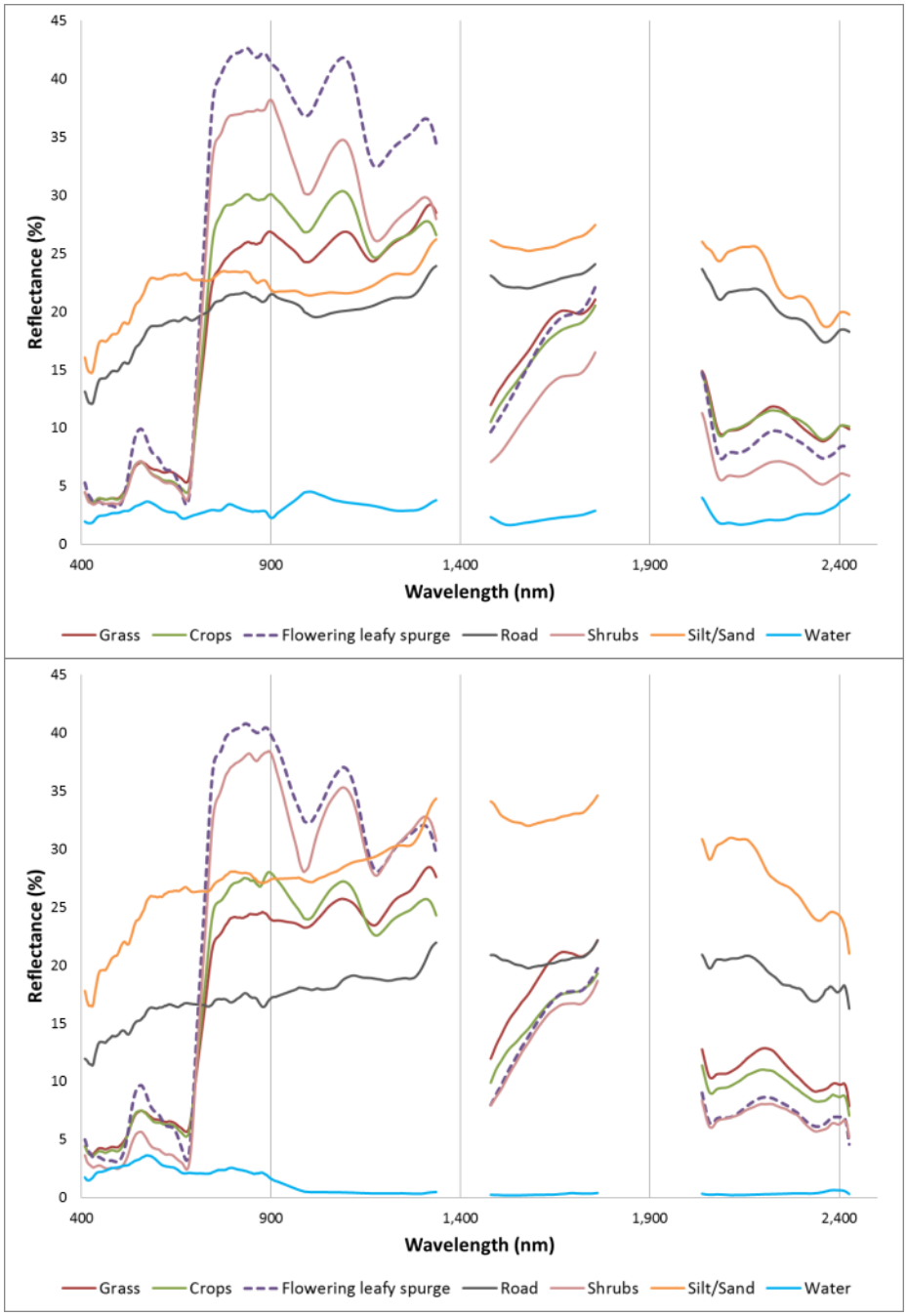

Figure 4-1: Comparison of flowering leafy spurge and other scene element spectra extracted from the AISA reflectance data cube showing the two flight lines (top and bottom) analyzed. A minimum of 5 pixels were averaged to generate the spectra.

The image flight lines were received already georeferenced and are accurate to within a pixel (Olaf Niemann, personal communication, May 17, 2013). Due to the lack of roads and buildings in the image scene a better accuracy estimate could not be achieved.

4.3 Stem Density Photograph Analysis

Interpolation of stem density estimates derived from the ground photographs corresponded to patches of different flowering leafy spurge densities identified by field observations using the AISA differential reflectance (Figures 4-2 and 4-3). Site 1 was selected for in-depth analyses because there were areas with differing spurge stem densities. At sites 1a and b there were a few low (1 - 14 stems m^{-2}) and medium (15 - 40 stems m^{-2}) density patches interspersed with large grassy areas, while at site 1c high density areas (> 40 stems m^{-2}) of leafy spurge were found. The latter were used to obtain a pure spectral endmember of leafy spurge from the image data. A positive relationship ($R^2 = 0.59$) was found between the actual and the predicted flowering stem counts as shown in Figure 4-4. The predicted values were slightly overestimated in some areas based on the regression line producing an RMSE of 14.19.

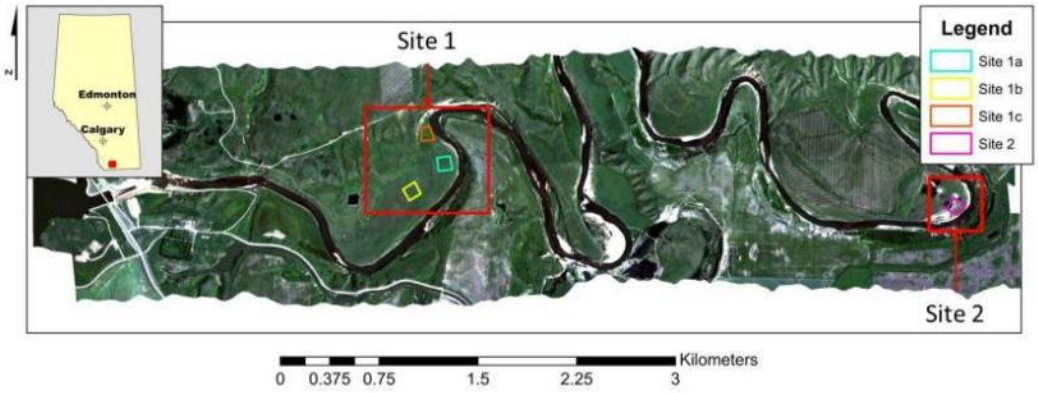

Figure 4-2: Study areas in the flats of the St. Mary River in southern Alberta overlaid on a true-colour composite AISA imagery (blue: band 24 (459 nm), green: band 64 (548 nm), and red: band 103 (638 nm)).

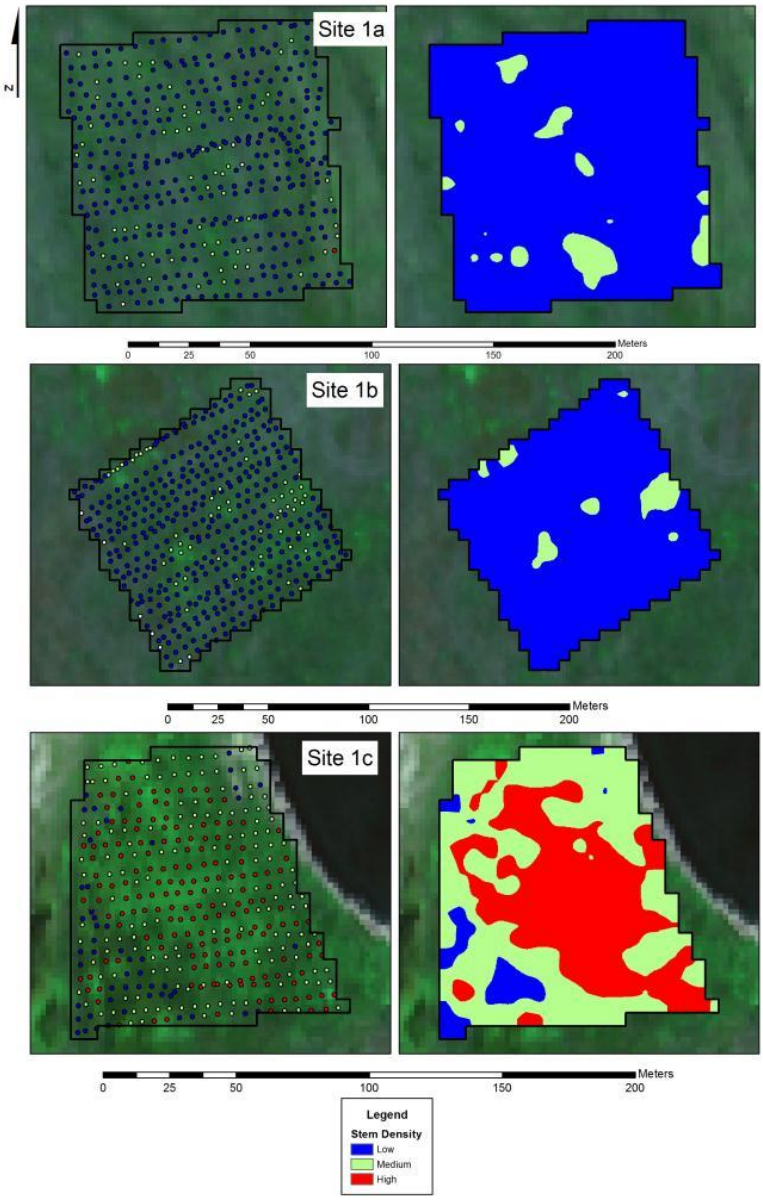

Figure 4-3: Predicted stem density estimates for all sample points extracted from ground photographs(left) and inverse-distance weighting interpolation of stem density estimates (right) at sites 1a, b and c overlaid on a true-colour composite AISA imagery (blue: band 24 (459 nm), green: band 64 (548 nm), and red: band 103 (638 nm))

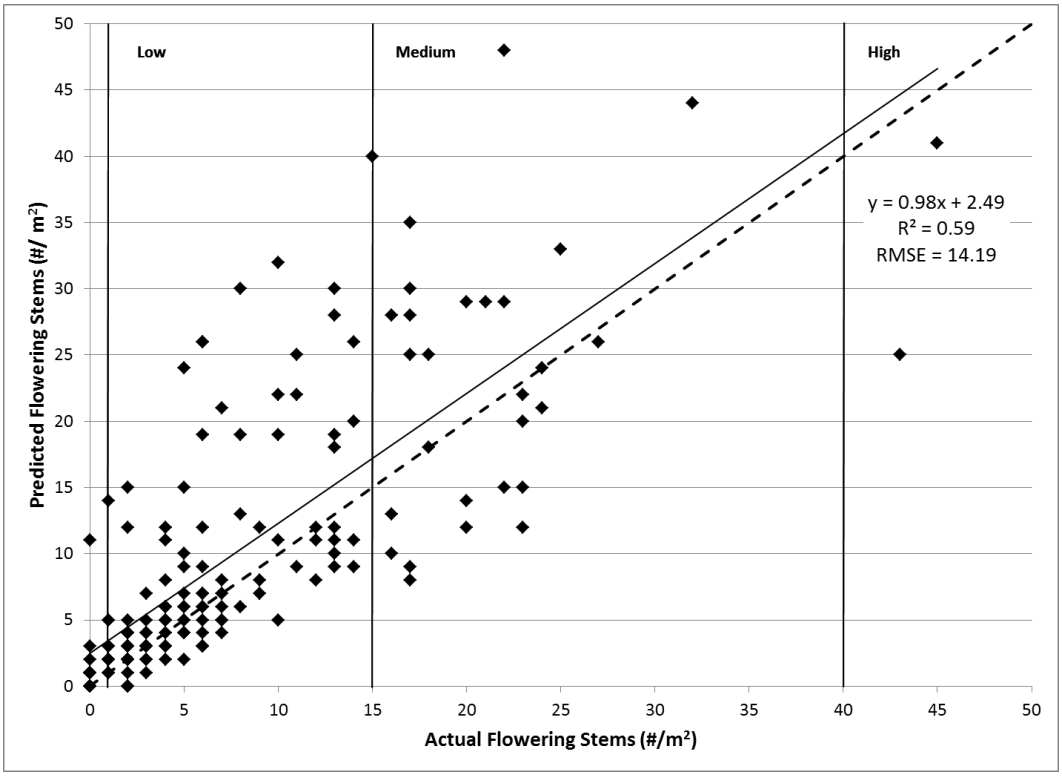

Figure 4-4: Relationship showing the number of actual flowering leafy spurge stems counted in the field and the predicted number of flowering stems derived from the ground-based photographs.

The ground photographs show promise for estimating stem density counts of leafy spurge in smaller patches as shown in Figure 4-3. Areas of shadow in the photographs affected the relationship that was established at Site 1a. HSB-threshold values were similar across all of the test sites and even with the shadowy areas in Site 1a taken into account and adjusted for a satisfactory relationship could not be established over all test sites. Shadowed areas of leafy spurge stems were not bright enough to be detected as leafy spurge using the HSB threshold values causing the RMSE to be high (14.19) in the

model. The airborne ortho photographs could have been used for this purpose, but due to blurring in some areas, they could not be widely used in this study for this purpose.

4.4 Ground-Spectra Analysis

Ground spectra were analyzed to determine if the spectral signature of flowering leafy spurge could be separated from other vegetative components in the scene. Qualitatively, the spectra generally showed separation in the spectral characteristics of flowering leafy spurge and the other potential scene elements present at the study site (Figure 4-5). Flowering leafy spurge stems showed higher reflectance in the visible (525 nm to 650 nm (yellow-green) and 650 nm to 700 nm ranges), the near-infrared (NIR) plateau (750 nm – 1300 nm) and the SWIR (1400 nm – 2500 nm) than the vegetative leafy spurge stems, grass, or other vegetation types. In the 1950 to 2250 nm region, flowering leafy spurge showed lower reflectance than the vegetative leafy spurge and the grass.

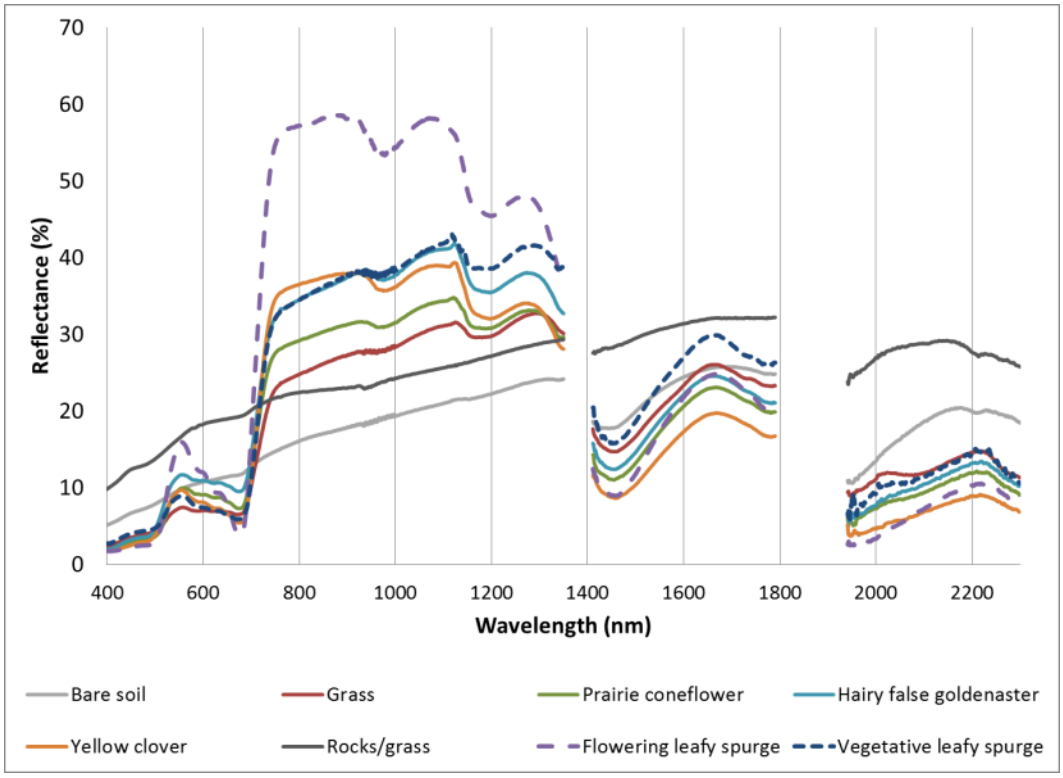

Figure 4-5: Average reflectance spectra of select ground target types. A minimum of 5 data points were averaged.

The ground spectra were examined but not used in the classification analysis due to the time lag of 18 days between the image data acquisition and the ground spectra collection. Collecting spectra closer to the time of the airborne data acquisition and a more intense ground campaign would improve the utility of the ground spectra.

4.5 Image Spectra Subsets

The original 492 bands (408 - 2500 nm) and two band subsets (495 - 668 nm and 409 - 794 nm) of imagery were used with the various algorithms to determine if all of the image data were needed for leafy spurge detection. The image data in the NIR and SWIR region showed spectra for the selected endmembers (Figure 4-6) with a magnitude in reflectance that is too high for vegetation towards the upper limit of the 1400-nm and 1800-nm ranges. Despite this problem, it was decided to test the full wavelength range as well as the reduced datasets eliminating either the SWIR or both the SWIR and NIR. With respect to the spectral subsets, the AISA image spectra subset of 409 nm - 794 nm showed the most difference in leafy spurge reflectance and compared to other plants and scene elements (Figure 4-7). It was comparative to the ground spectra collected in terms of the shape (Figure 4-8). The 495 - 668 nm range was selected to test the wavelengths that covered the spectral peak shown in the green/yellow range (Figure 4-7). Due to the presence of both vegetative and flowering leafy spurge in the 2-m AISA pixel, the reflectance extracted from the AISA imagery in the VNIR is therefore lower compared with the ground (Figure 4-8).

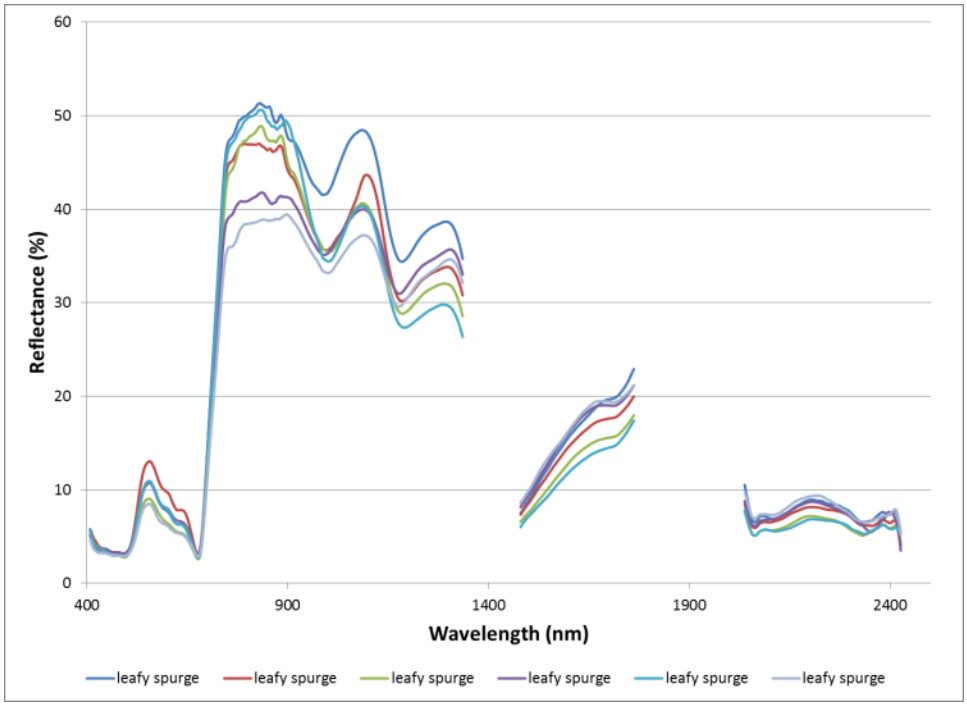

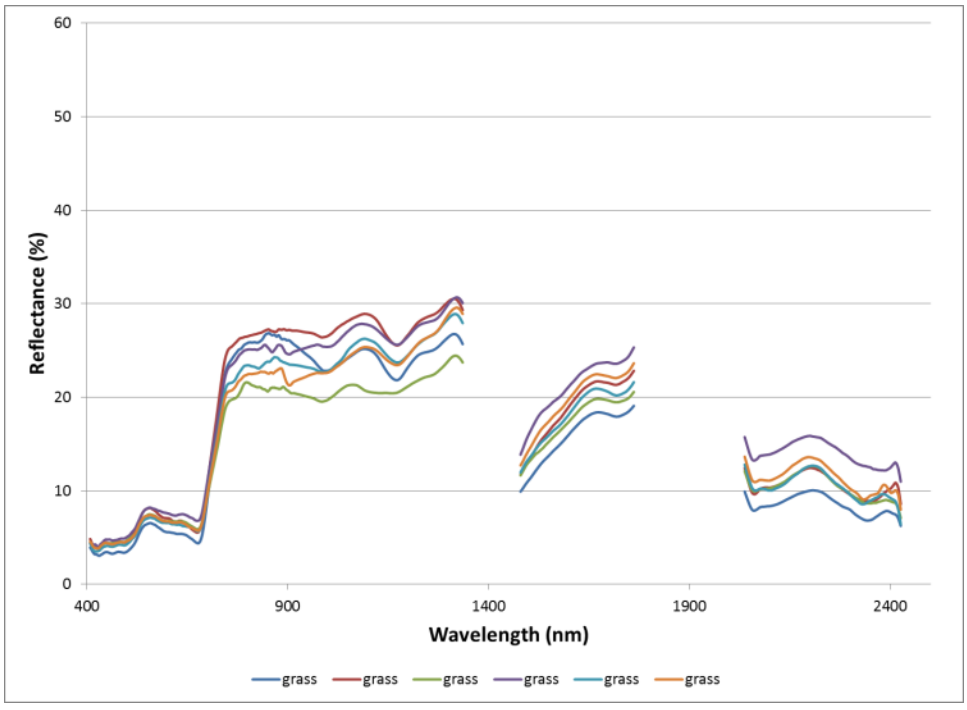

Figure 4-6: Endmembers of flowering leafy spurge (top) and grass (bottom) selected throughout the image area for use with classification algorithms.

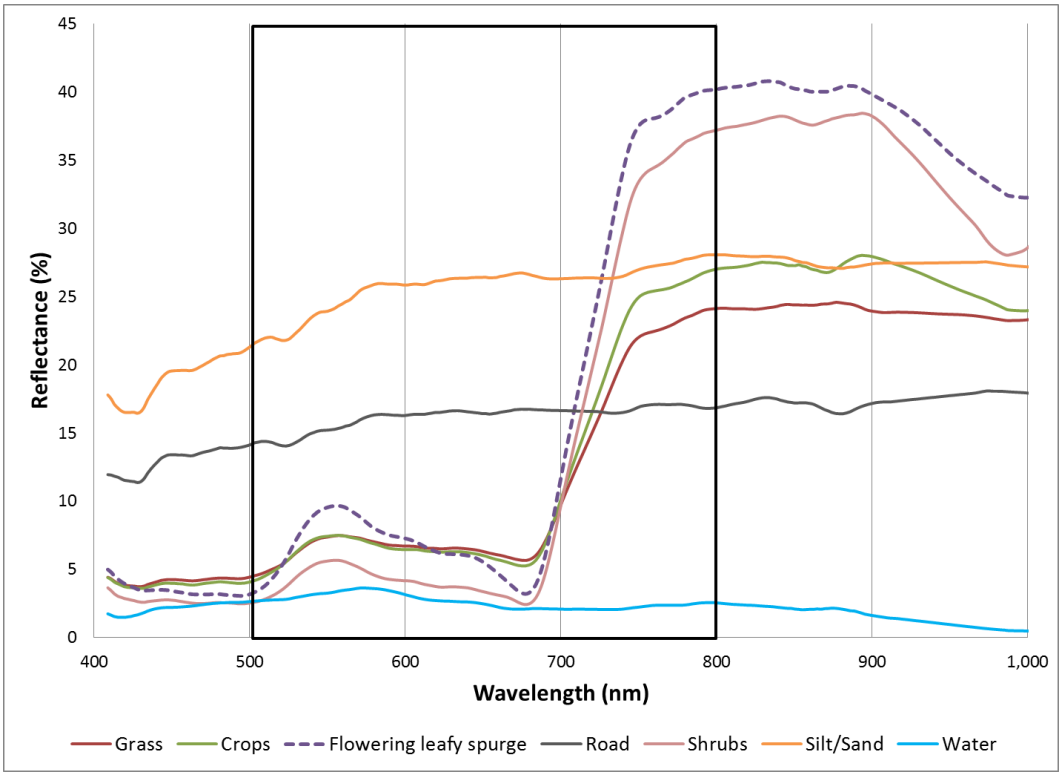

Figure 4-7: Comparison of flowering leafy spurge and other scene element spectra extracted from the AISA reflectance data cube. The black box shows the wavelengths between 500 nm and 800 nm to highlight the spectral peak shown in the green/yellow range. Minimum of 5 data points were averaged to account for spectral variability throughout the image.

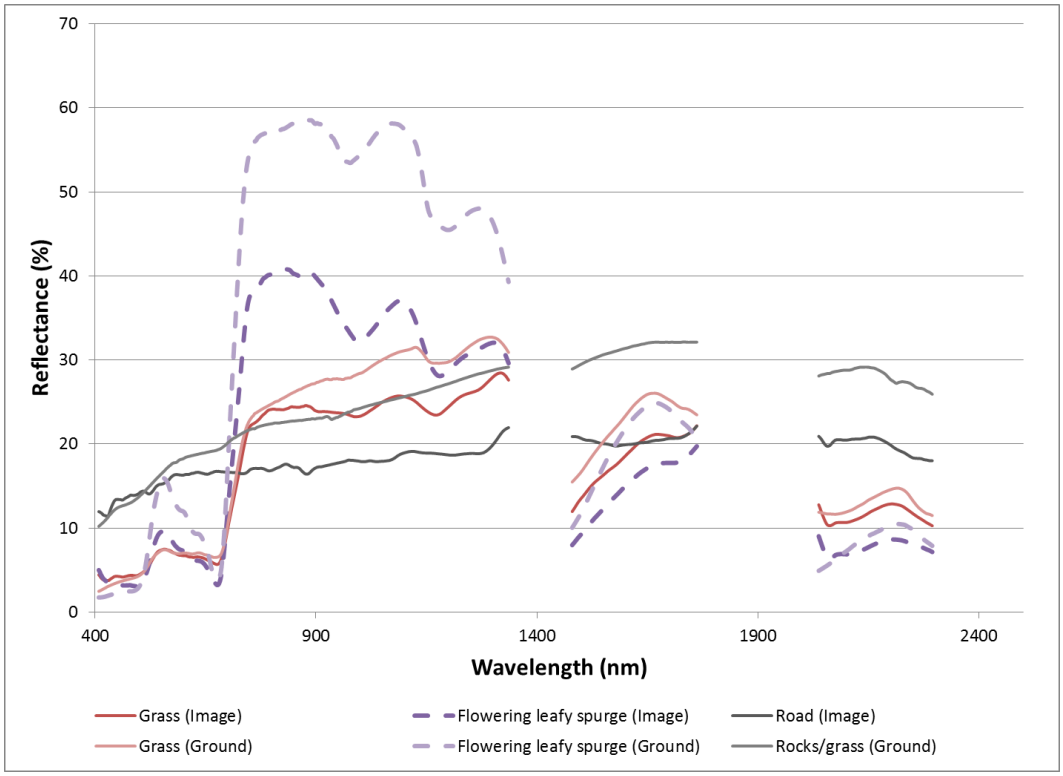

Figure 4-8: Comparison of scene element spectra extracted from the AISA reflectance data cube and the ground spectra collected. Minimum of 5 data points were averaged.

Due to higher magnitude of the image spectra in the NIR and SWIR ranges in the image compared to the ground data, the bands in those wavelength ranges were not included in some of the image analysis. Removing the NIR and SWIR bands allowed for better classification accuracies. Overall accuracy was 46.8 - 86.7 % with the NIR and SWIR and 76.8 – 85.0 % without the NIR AND SWIR. Similarly, Stitt et al. (2006) found that using the mid-SWIR band (1550 - 1750 nm) in multispectral images decreased the classification accuracies. Based on this fact and what appeared to be the issues in the

image data in this region (see Section 4.2), a different spectral dataset could potentially be used to test the bands in this particular wavelength range.

4.6 Image Classification

4.6.1 Spectral Angle Mapper

The three different image classifiers and different image band sets showed varying classifications results. The use of the SAM classifier and the reflectance data from the three-band sets tended to overestimate the leafy spurge present in the scene compared to the known areas of leafy spurge patches identified on the ground data (Figures 4-9, 4-10 and 4-11).

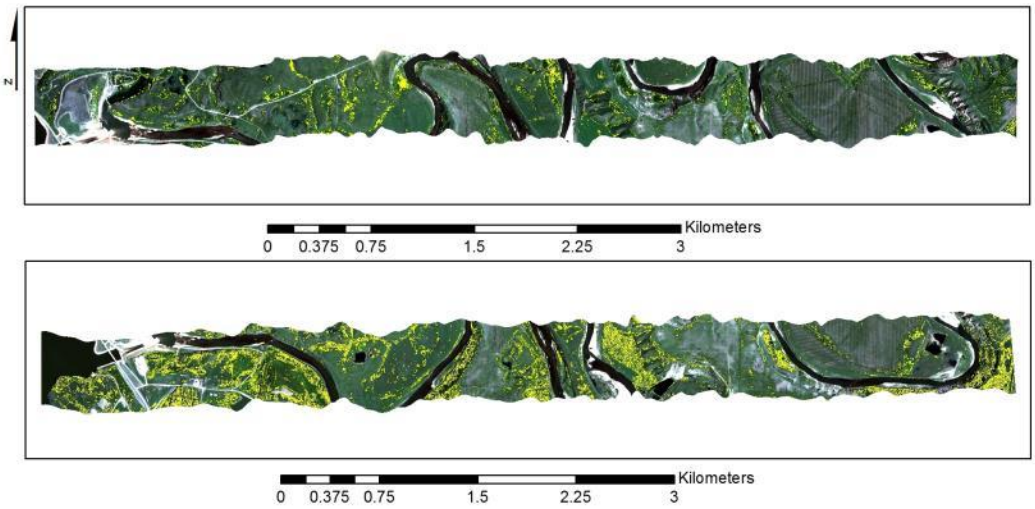

Figure 4-9: SAM classifier using the full VNIR and SWIR spectral wavelength range overlaid on an AISA true-colour composite image with flightline 1616 (top) and flightline 1610 (bottom) in (blue: band 24 (459 nm), green: band 64 (548 nm), and red: band 103 (638 nm)). Yellow areas indicate the presence of flowering leafy spurge.

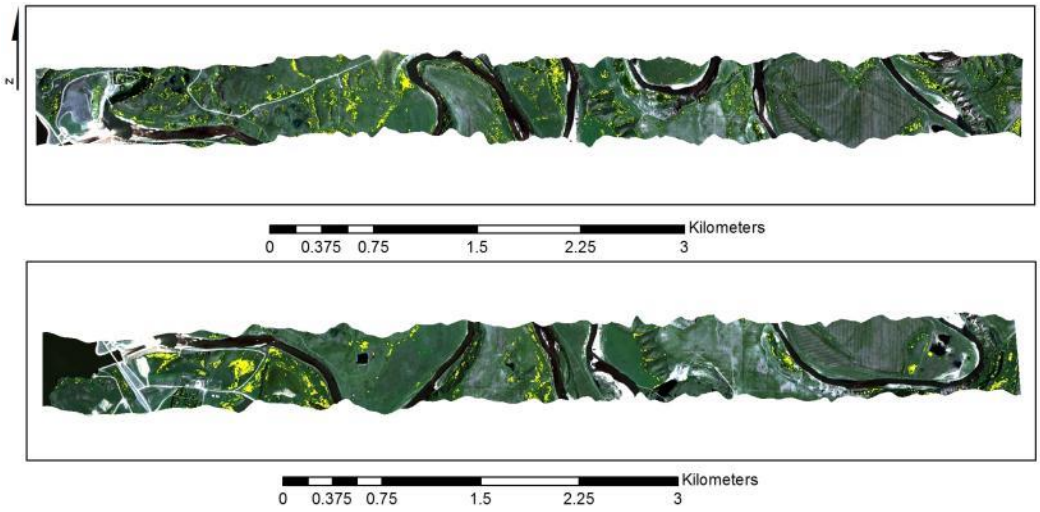

Figure 4-10: SAM classifier using the 409 nm – 794 nm spectral wavelength range overlaid on an AISA true-colour composite image with flightline 1616 (top) and flightline 1610 (bottom) in (blue: band 24 (459 nm), green: band 64 (548 nm), and red: band 103 (638 nm)). Yellow areas indicate the presence of flowering leafy spurge.

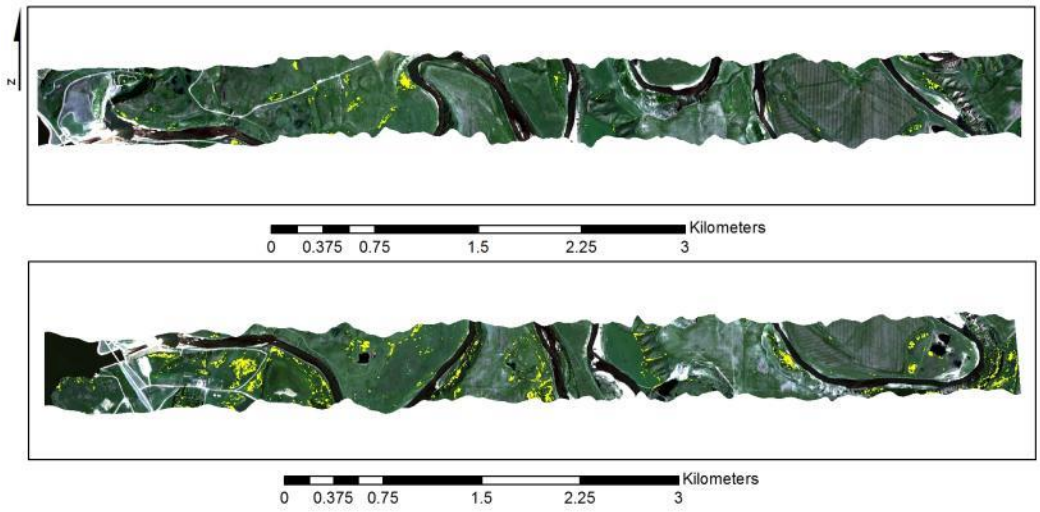

Figure 4-11: SAM classifier using the 495 nm – 668 nm spectral wavelength range overlaid on an AISA true-colour composite image with flightline 1616 (top) and flightline 1610 (bottom) in (blue: band 24 (459 nm), green: band 64 (548 nm), and red: band 103 (638 nm)). Yellow areas indicate the presence of flowering leafy spurge.

O'Neill et al. (2000) found the best results using a combination of the MNF transform and the SAM algorithm (Figures 4 -12, 4-13, and 4-14) compared to using the SAM classifier on non-transformed data. The original and image subsets were transformed using MNF. The full spectral range and 450 nm - 668 nm showed the best results in comparison to known areas and validation sites. The 409 nm - 794 nm range tended to overestimate the leafy spurge (34 % found in the low density), and there was confusion with the trees/shrubs in the image. The non-transformed data tended to overestimate the leafy spurge for all of the spectral ranges tested.

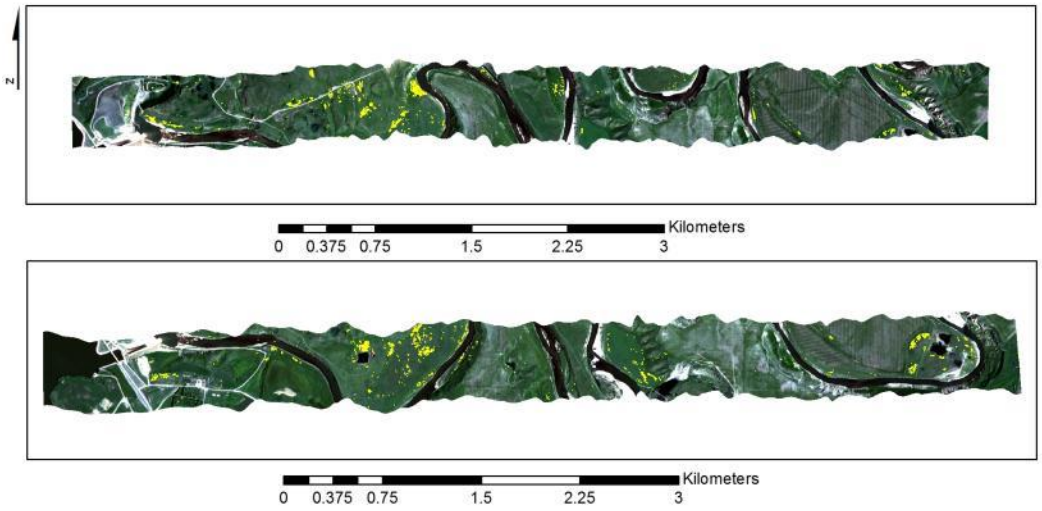

Figure 4-12: SAM classifier using the full VNIR and SWIR spectral wavelength range with the MNF transform overlaid on an AISA true-colour composite image with flightline 1616 (top) and flightline 1610 (bottom) in blue (band 24 (459 nm), green (band 64 (548 nm), and red (band 103 (638 nm)). Yellow areas indicate the presence of flowering leafy spurge.

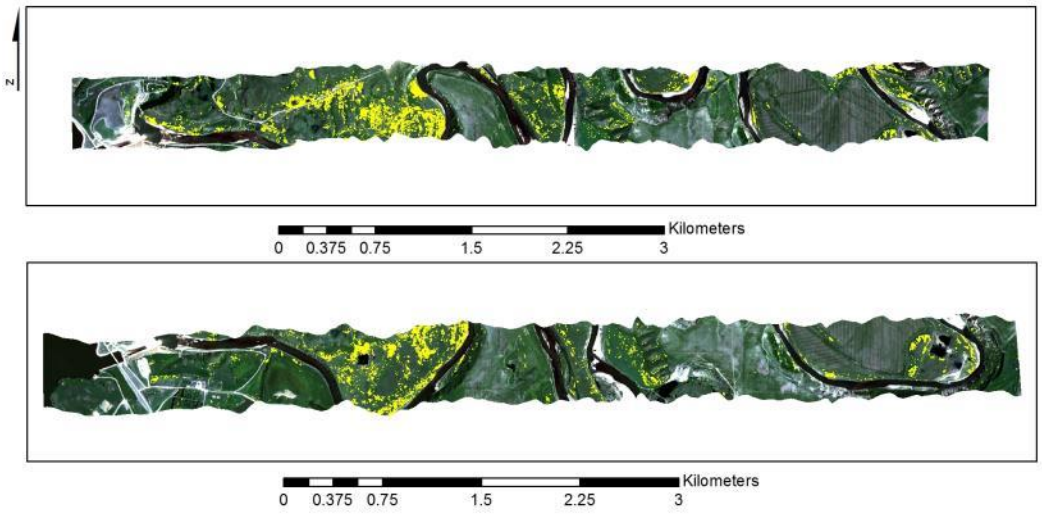

Figure 4-13: SAM classifier using the 409-nm – 794-nm spectral wavelength range with the MNF transform overlaid on an AISA true-colour composite image with flightline 1616 (top) and flightline 1610 (bottom) in blue: band 24 (459 nm), green: band 64 (548 nm), and red: band 103 (638 nm). Yellow areas indicate the presence of flowering leafy spurge.

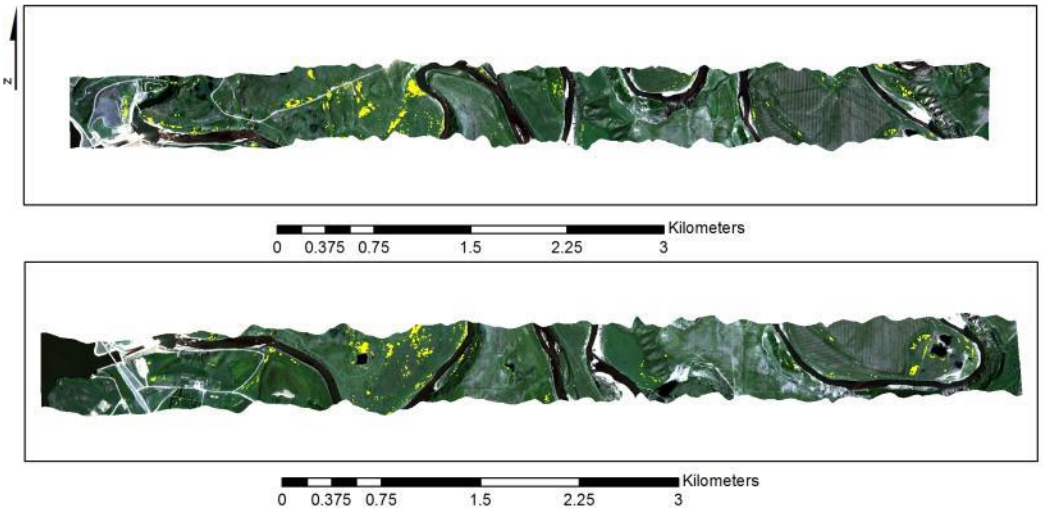

Figure 4-14: SAM classifier using the 495-nm – 668-nm spectral wavelength range with the MNF transform overlaid on an AISA true-colour composite image with flightline 1616 (top) and flightline 1610 (bottom) in blue: band 24 (459 nm), green: band 64 (548 nm), and red: band 103 (638 nm). Yellow areas indicate the presence of flowering leafy spurge.

4.6.2 Mixture-Tuned Match Filtering

The MTMF classifier using the flowering leafy spurge endmember from Figure 4-6 had the highest accuracy and the best visual results over the whole spectral range compared to the SAM and MESMA classifiers (Figures 4-15, 4-16, and 4-17). The overall increased performance is most likely due to the MNF preprocess step removing noise and decorrelating data that is needed to implement the MTMF. There was some underestimation of the denser areas of leafy spurge in the image. The spectral ranges of 409 - 794 nm and 495- 668 nm showed more promise for detecting these areas. The difficulty in using this method is in selecting a threshold without accepting too many false positives (Figure 4-18). The threshold values used in this study did result in some known areas of high-density beingmissed in the classifications.

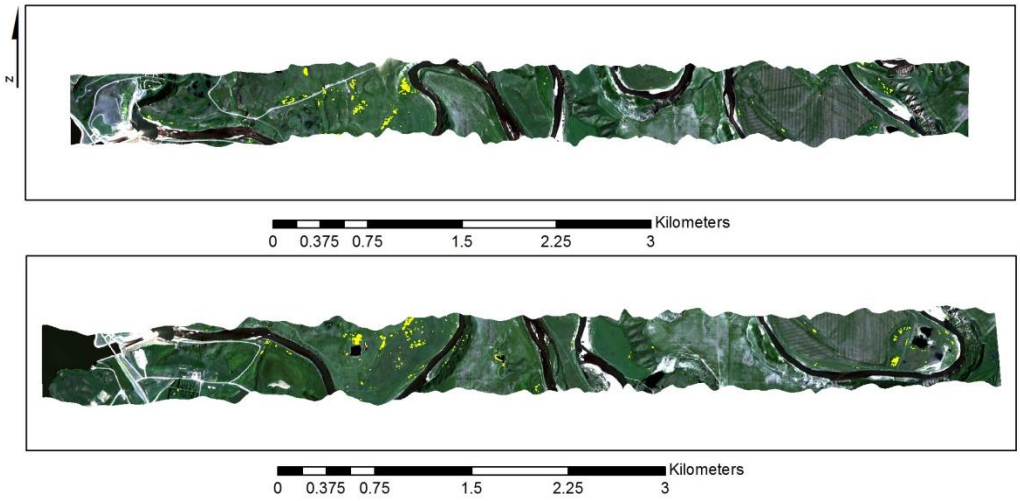

Figure 4-15: MTMF classifier using the full VNIR and SWIR spectral wavelength range overlaid on an AISA true-colour composite image with flightline 1616 (top) and flightline 1610 (bottom) in blue (band 24 (459 nm)), green (band 64 (548 nm)), and red (band 103 (638 nm)). Yellow areas indicate the presence of flowering leafy spurge.

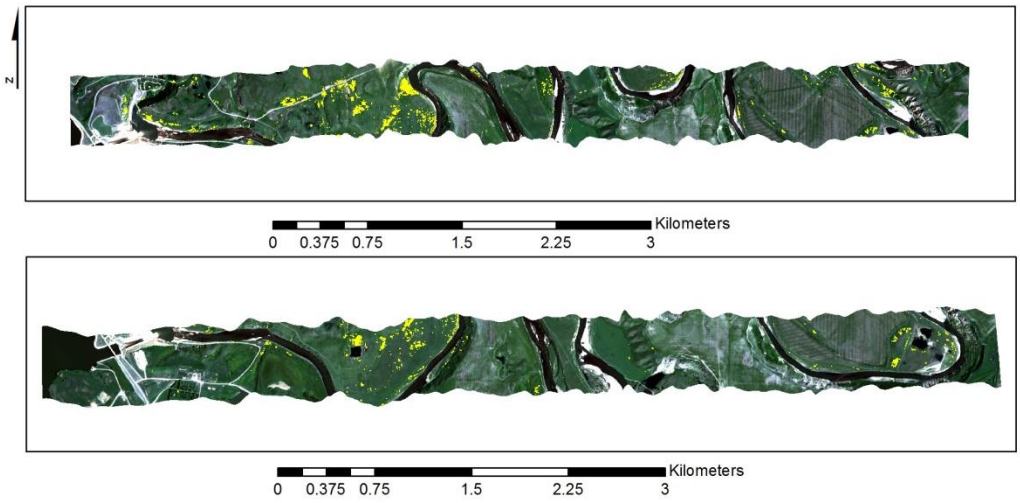

Figure 4-16: MTMF classifier using the 409-nm – 794-nm spectral wavelength range overlaid on an AISA true-colour composite image with flightline 1616 (top) and flightline 1610 (bottom) in blue: band 24 (459 nm), green: band 64 (548 nm), and red: band 103 (638 nm). Yellow areas indicate the presence of flowering leafy spurge.

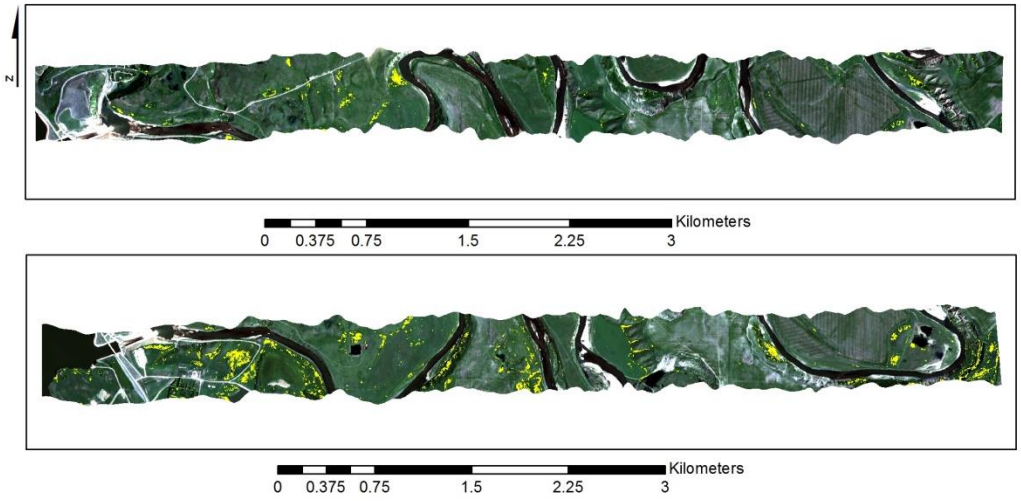

Figure 4-17: MTMF classifier using the 495-nm – 668-nm spectral wavelength range overlaid on an AISA true-colour composite image with flightline 1616 (top) and flightline 1610 (bottom) in blue: band 24 (459 nm), green: band 64 (548 nm), and red: band 103 (638 nm). Yellow areas indicate the presence of flowering leafy spurge.

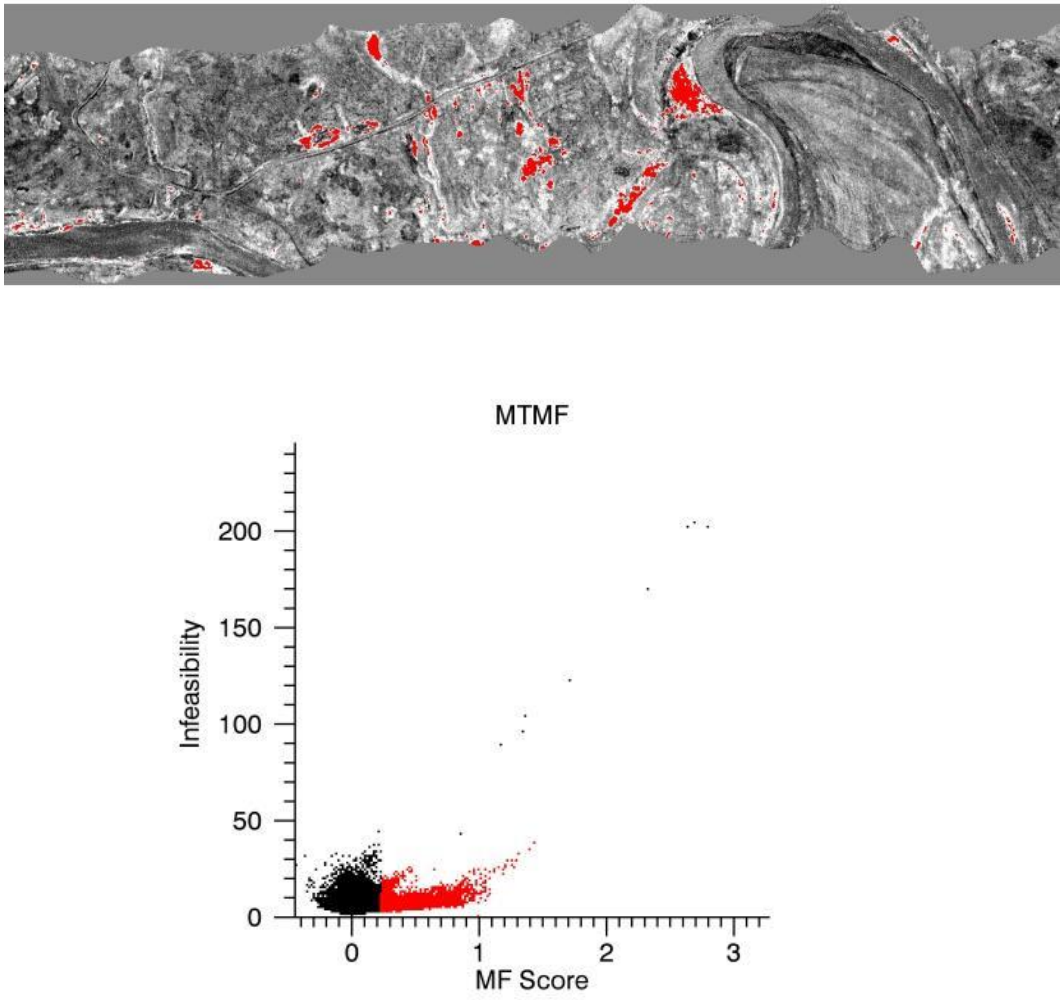

Figure 4-18: Sample of the MF score results (top) and scatterplot (bottom) showing the MTMF threshold overlaid. The red data points indicate the areas selected by the threshold for the MTMF classifier.

4.6.3 Multiple Endmember Spectral Mixture Analysis

For MESMA, a three-endmember model was selected for use and the endmembers selected were flowering leafy spurge, grass, and then a generalized class of other grassland vegetation. A threshold of 50 % for the fraction cover map was selected

in the areas containing the flowering leafy spurge. In general, MESMA overestimated the leafy spurge presence for the full band set and band subsets considered. Confusion between areas of trees/shrubs was evident in (Figures 4-19 and 4-20). This may be attributed to an incomplete image endmember dataset as a result of complexity of the grassland scene (Figures 4-21 and 4-22).

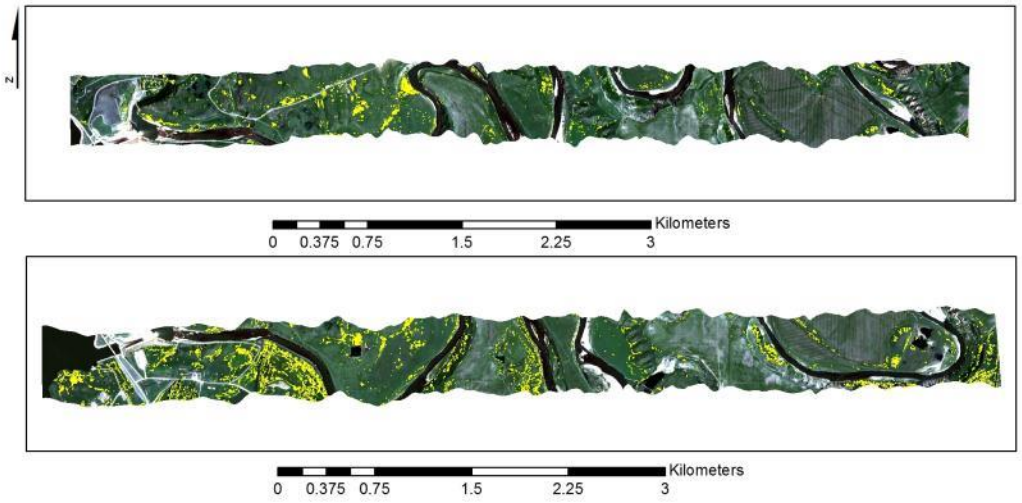

Figure 4-19: MESMA classifier using the 409-nm – 794-nm spectral wavelength range overlaid on an AISA true-colour composite image with flightline 1616 (top) and flightline 1610 (bottom) in blue: band 24 (459 nm), green: band 64 (548 nm), and red: band 103 (638 nm). Yellow areas indicate the presence of flowering leafy spurge at a > 50-% fractional cover (density).

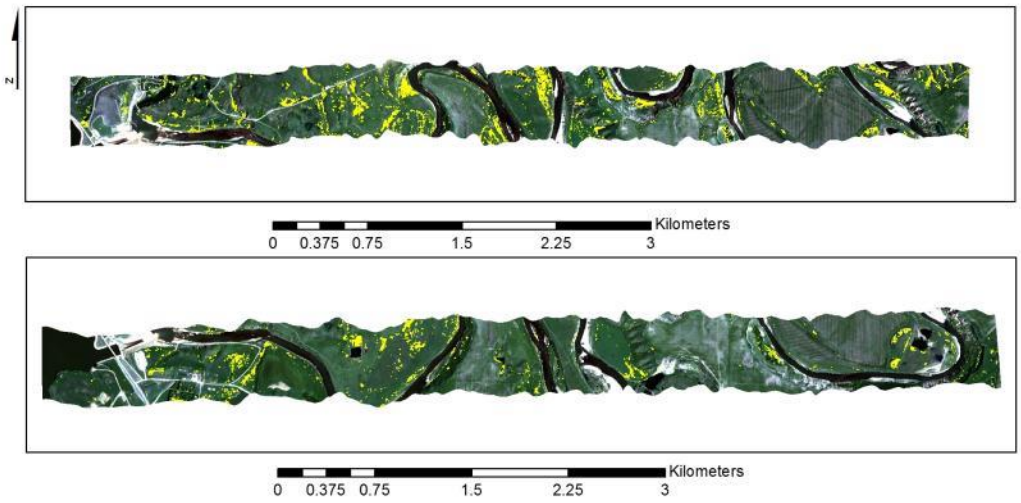

Figure 4-20: MESMA classifier using the 495-nm – 668-nm spectral wavelength range overlaid on an AISA true-colour composite image with flightline 1616 (top) and flightline 1610 (bottom) in blue: band 24 (459 nm), green: band 64 (548 nm), and red: band 103 (638 nm). Yellow areas indicate the presence of flowering leafy spurge.

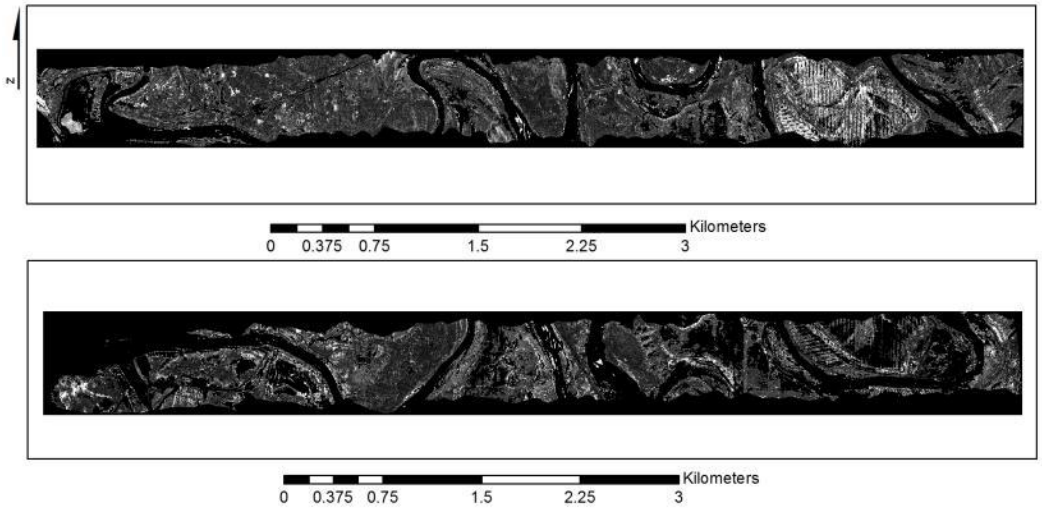

Figure 4-21: RMSE image from the MESMA classifier using the 409-nm – 794-nm spectral wavelength range. White pixels in the image have a higher RMSE value, showing higher residuals or areas where there were no endmembers used from the MESMA model.

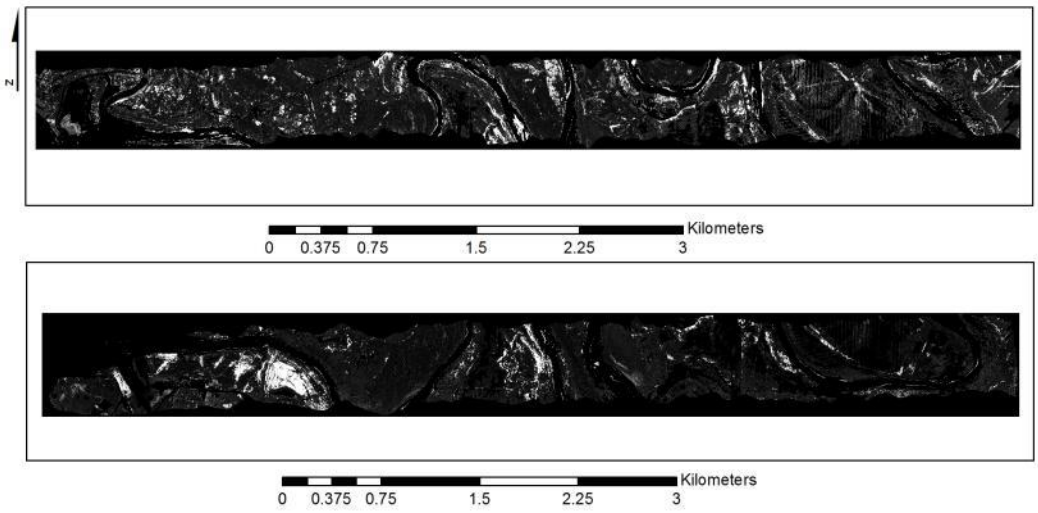

Figure 4-22: RMSE image from the MESMA classifier using the 495-nm – 668-nm spectral wavelength range. White pixels in the image have a higher RMSE value, showing higher residuals or areas where there were no endmembers used from the MESMA model.

The results of the MTMF and MESMA approaches were similar to those of the SAM in terms of identifying the location of leafy spurge using the 495-nm – 668-nm range and the MNF transform (Figures 4-23, 4-24, and 4-25). The difference is the fact that MESMA provides a relative abundance measure and MTMF and SAM only indicate presence or absence of leafy spurge. All the classifiers were able to detect leafy spurge with MESMA being superior in detecting areas of medium density leafy spurge (44.2 %) with some overestimation, while the MTMF approach uses an arbitrary threshold for the MF and infeasibility scores to avoid false positives in the resulting classification and, therefore, appears to miss areas of higher density when compared to the other two classifiers.

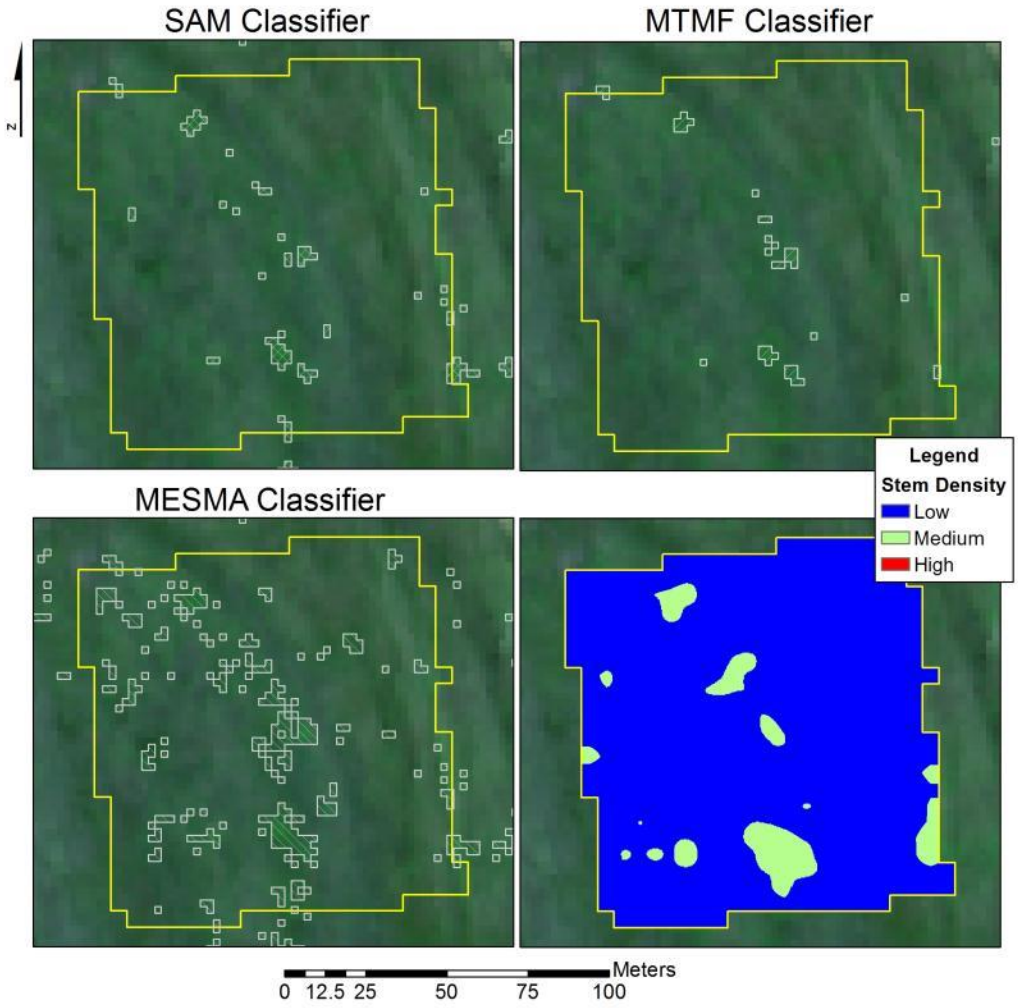

Figure 4-23: Comparison of the SAM, MTMF, and MESMA classifications using the spectral range of 495 nm - 668 nm and stem density estimates from ground-based photographs of Site 1a overlaid on an AISA true-colour composite image (blue: band 24 (459 nm), green: band 64 (548 nm), and red: band 103 (638 nm)).

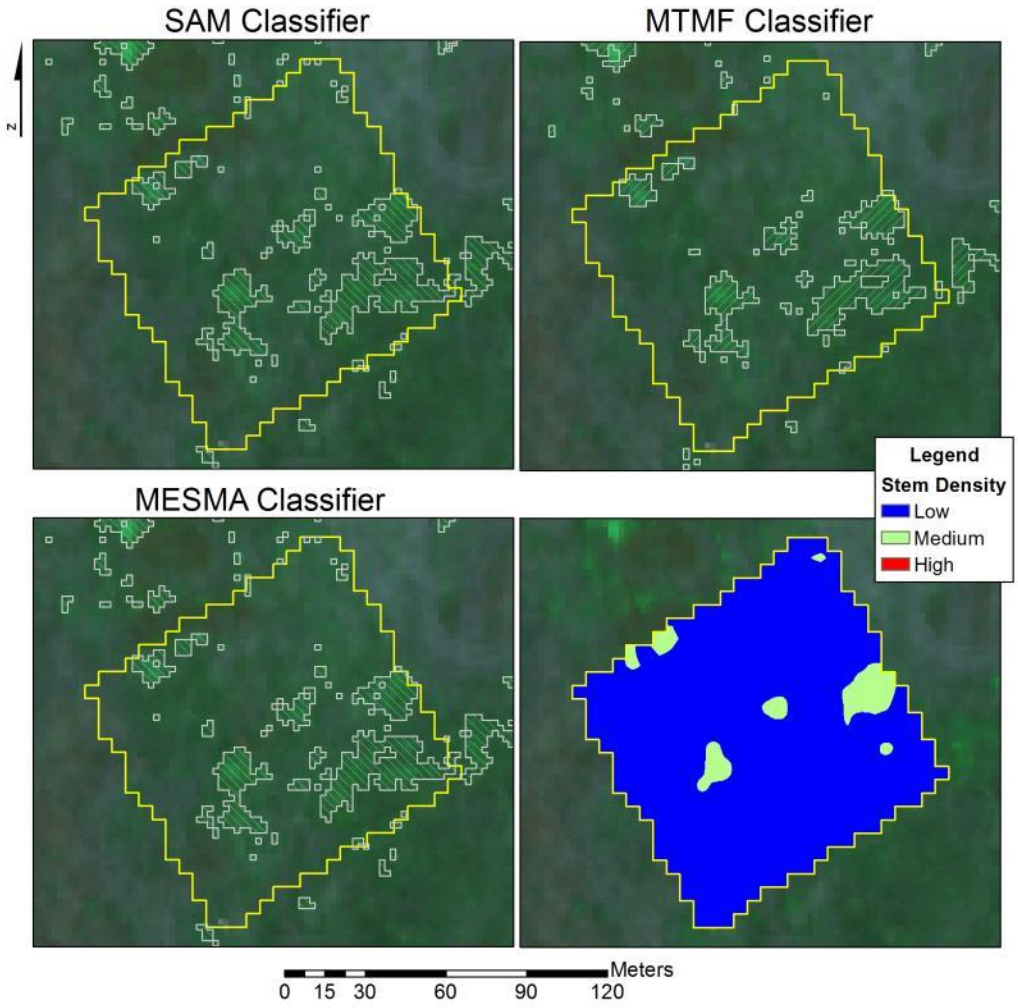

Figure 4-24: Comparison of SAM, MTMF, and MESMA classifications using the spectral range of 495 nm - 668 nm and stem density estimates from ground-based photographs of Site 1b overlaid on an AISA true-colour composite image (blue: band 24 (459 nm), green: band 64 (548 nm), and red: band 103 (638 nm)).

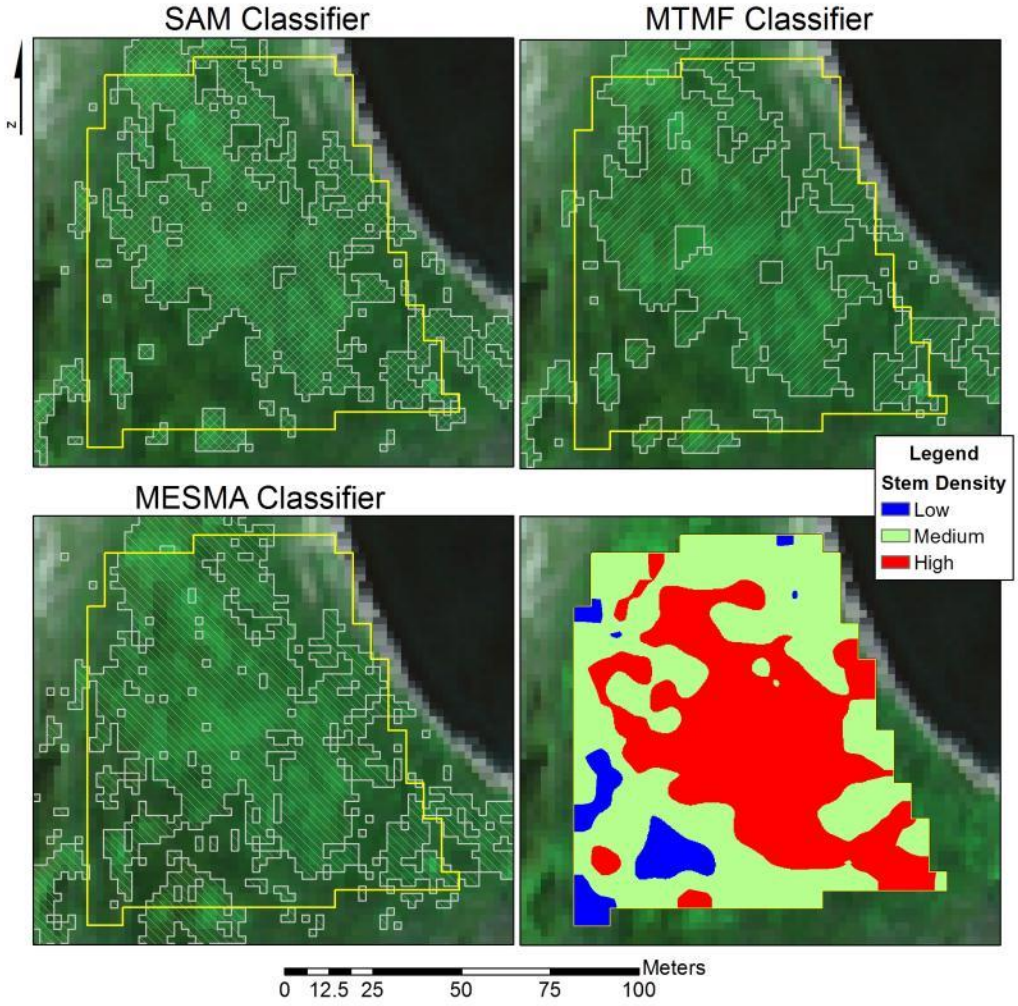

Figure 4-25: Comparison of SAM, MTMF, and MESMA classifications using the spectral range of 495 nm - 668 nm and stem density estimates from ground-based photographs of Site 1c overlaid on an AISA true-colour composite image (blue: band 24 (459 nm), green: band 64 (548 nm), and red: band 103 (638 nm)).

4.7 Map Validation

The classification results were validated with the stem density measurements collected on July of 2010 using a log-linear analysis method as discussed in Chapter 3 (Figure 4-26). With all three classifiers, high-density leafy spurge patches (> 40 stems m^{-2}) were detected with an accuracy of 80 % (SAM) or higher (MTMF and MESMA). Between 30 % - 45 % of the medium-density patches (15 – 40 stems m^{-2}), were identified while detection of patches of low density (< 15 stems m^{-2}) was less certain with less than 10 % of the sites being identified.

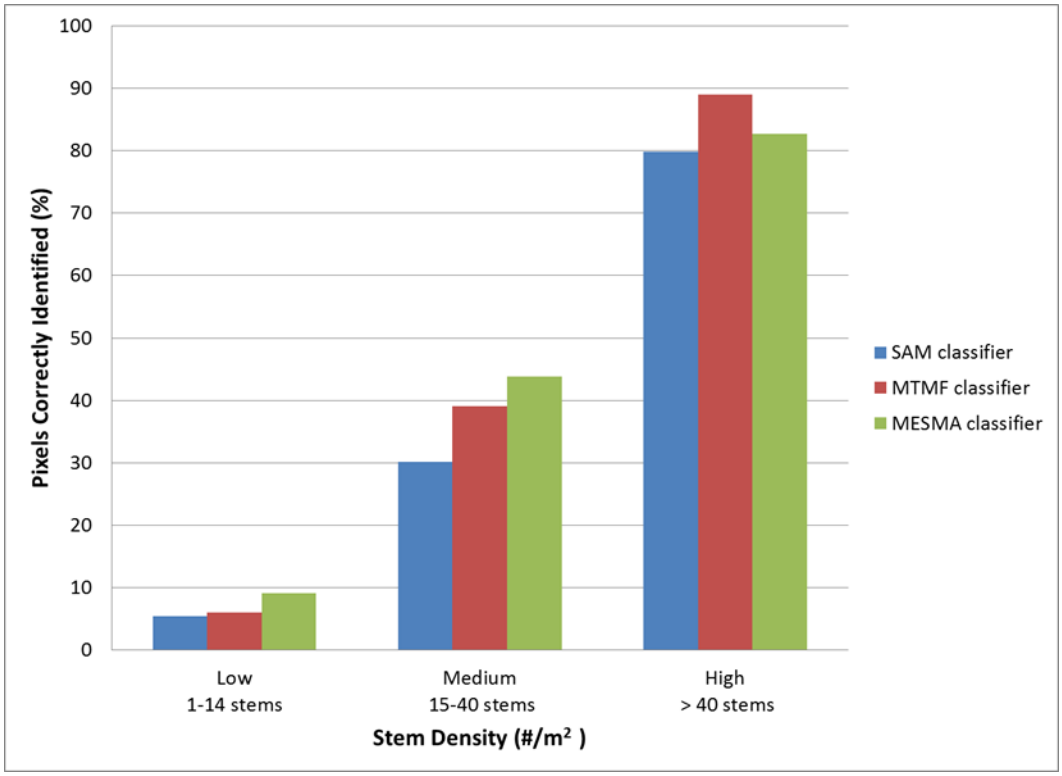

Figure 4-26: Results of log-linear analysis used to determine the average percentage of pixels correctly identified as high, medium, or low density leafy spurge using the three classifiers, SAM, MTMF, and MESMA at sites 1a,1b, and 1c using the spectral range of 495 nm - 668 nm.

Further validation of the remote sensing derived leafy spurge maps was conducted using GPS coordinates collected in the study area in October of 2011 and the classified maps. The initial validation data were collected during the fall when there were no flowering stems present, making it difficult to distinguish all of the stems present in the area. Figure 4-27 shows classification examples with the GPS coordinates of leafy spurge locations overlaid. The percentage of pixels found in the image at the GPS sites in Figure 4-27 that contained leafy spurge was low at 22.9 % for the SAM, 31.3 % for MTMF, and 33.7 % for MESMA for the spectral range of 495 nm - 668 nm. Results were similar between all three classification approaches. The pattern of the leafy spurge points collected and those identified in the image were similar but offset. This offset is probably due to the error between the GPS used to collect the points in the field and the geocorrection of the image. The GPS was only accurate to between 2 m to 4 m in the field, which is greater than the pixel size of the imagery used.

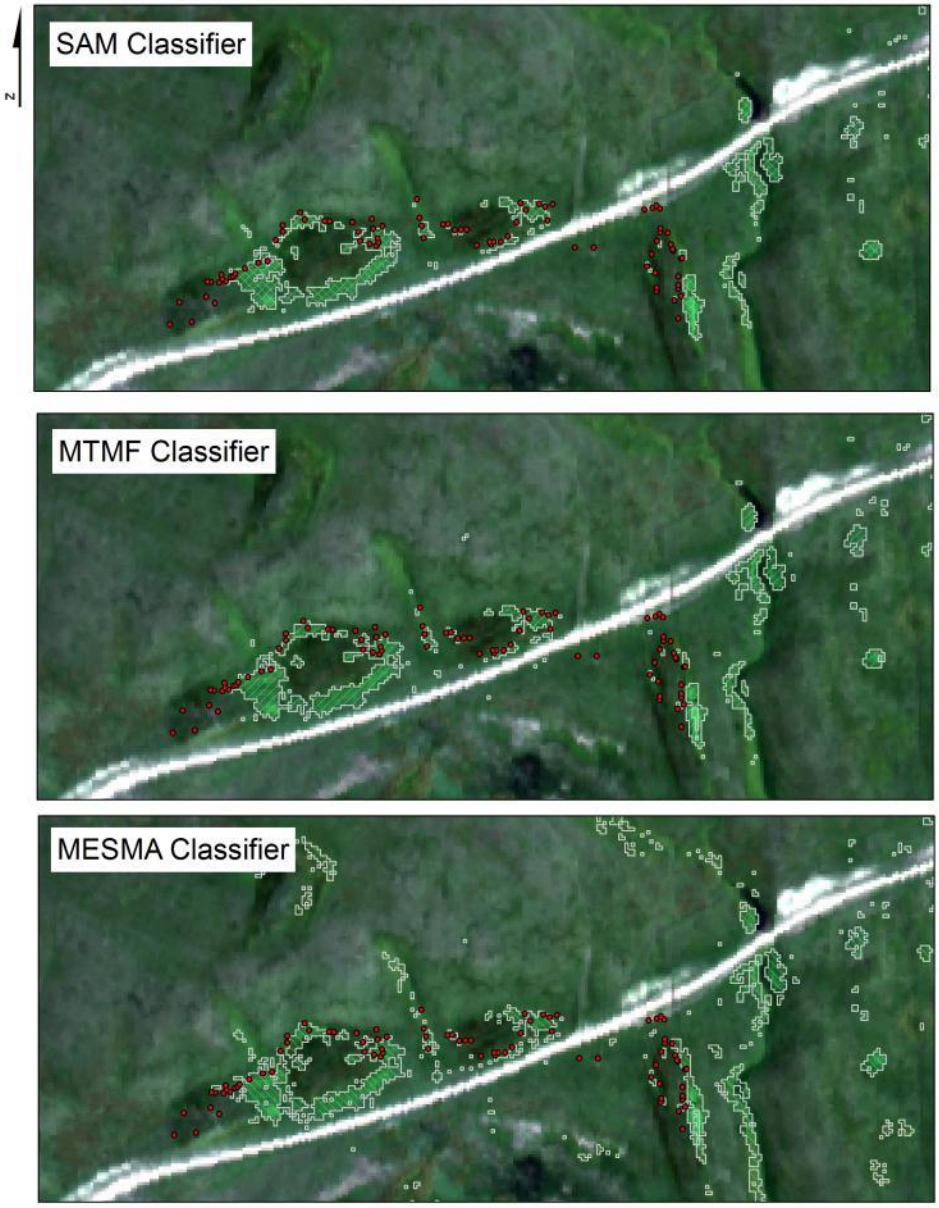

Figure 4-27: Results of the SAM (top), MTMF (middle), and MESMA (bottom) classification approaches using the spectral range of 495 nm - 668 nm overlaid on an AISA imagery (blue: band 24 (459 nm), green: band 64 (548 nm), and red: band 103 (638 nm)). Red dots indicate areas of leafy spurge observed in the field in October 2011.

A subsequent validation campaign was conducted in July, 2012 to confirm areas of flowering leafy spurge identified in the classified images (Figure 4-28). For this purpose, six areas as identified of leafy spurge in the imagery were selected in the field. Two areas, validation sites 4 and 6, appeared on a first glance to be incorrectly identified as leafy spurge in the classified image. However, examination of these areas in 2012 showed either dead leafy spurge stems or vegetative stems (Figure 4-29). The land owners indicated that both areas were sprayed with herbicides or grazed in previous years to control the leafy spurge. This suggests that in these areas was indeed present at the time of image collection in 2010 and were correctly identified with the classification procedure.

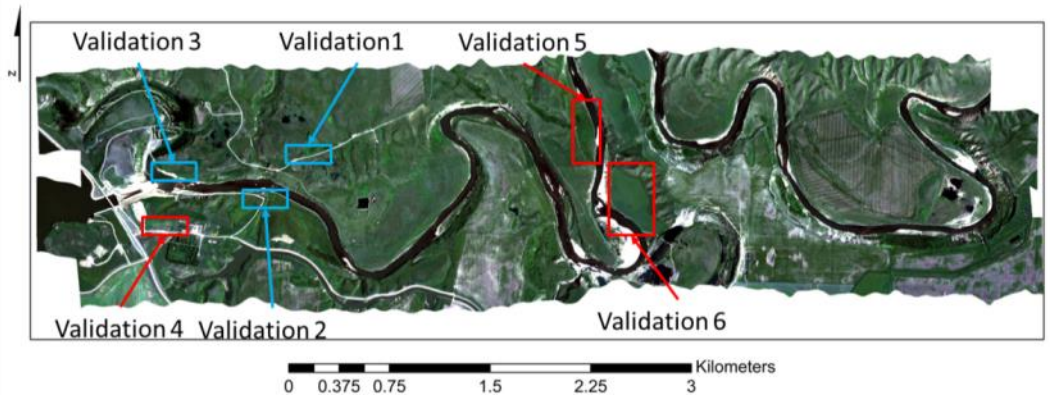

Figure 4-28: AISA imagery showing sites selected for validation in July, 2012. Blue boxes indicate sites where polygon and/or stem densities were acquired in the field. Red boxes indicate unknown areas of potential false positives selected for ground validation.

Figure 4-29: Field photographs showing the presence of dead leafy spurge stems as indicated by the red box located at the validation site 4 (left) and the presence of vegetative leafy spurge stems at the validation site 6 (right) as indicated by the red box.

At the validation sites 1, 2, 3, and 5 where leafy spurge was detected in the classified images, the weed was found to be present (Figures 4-30, 4-31, 4-32, and 4-33). Additional stem density counts following the same procedure as the initial field campaign in July of 2010 were made at two of the sites in the summer of 2012 (Table 4-1). Percentages were calculated based on the number of points collected that had leafy spurge present. The points were mostly in the medium stem density range. For these reasons, the low density patches found are most likely due to two years of vegetation growth between the image acquisition date and the field data collection date.

Table 4-1: July 2012 validation results.

Validation Site	Classifier	Wavelength (nm)	Validation	
			Pixel Count	(%)
1	SAM	409 - 2500	11/16	68.75
3			10/16	62.5
1		409 - 794	9/16	56.25
3			8/16	50
1		495 - 668	6/16	37.5
3			5/16	31.25
1	SAM MNF	409 - 2500	7/16	43.75
3			6/16	37.5
1		409 - 794	8/16	50
3			10/16	62.5
1		495 - 668	9/16	56.25
3			4/16	25
1	MTMF	409 - 2500	4/16	25
3			3/16	18.75
1		409 - 794	8/16	50
3			6/16	37.5
1		495 - 668	9/16	56.25
3			5/16	31.25
1	MESMA	409 - 794	7/16	43.75
3			6/16	37.5
1		495 - 668	9/16	56.25
3			5/16	31.25

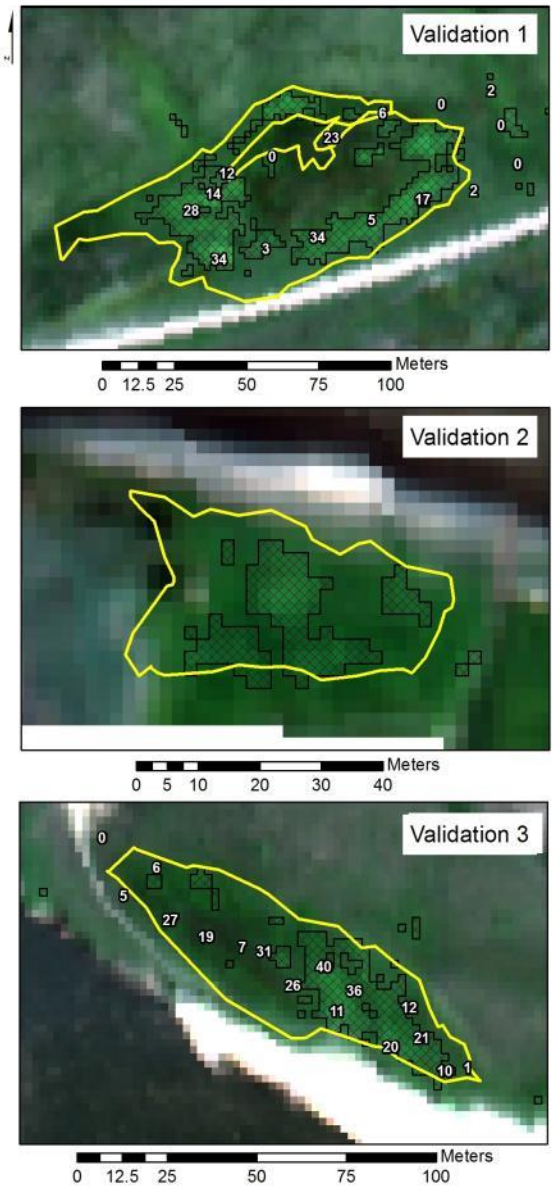

Figure 4-30: Results of the SAM classification approach using the spectral range of 495 nm - 668 nm at validation sites 1 (top), 2 (middle), and 3 (bottom) with reference stem density counts overlaid on an AISA image (blue: band 24 (459 nm), green: band 64 (548 nm), and red: band 103 (638 nm)). The yellow polygons show the areas ground surveyed in July of 2012.

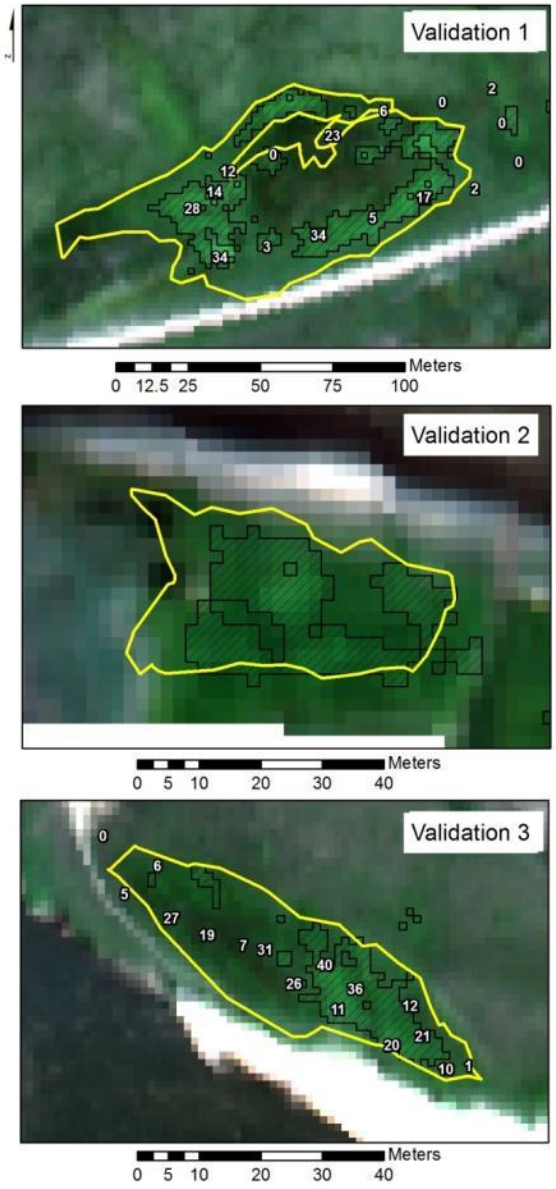

Figure 4-31: Results of the MTMF classification approach using the spectral range of 495 nm - 668 nm at validation sites 1 (top), 2 (middle), and 3 (bottom) with reference stem density counts overlaid on an AISA image (blue: band 24 (459 nm), green: band 64 (548 nm), and red: band 103 (638 nm)). The yellow polygons show the areas ground surveyed in July of 2012.

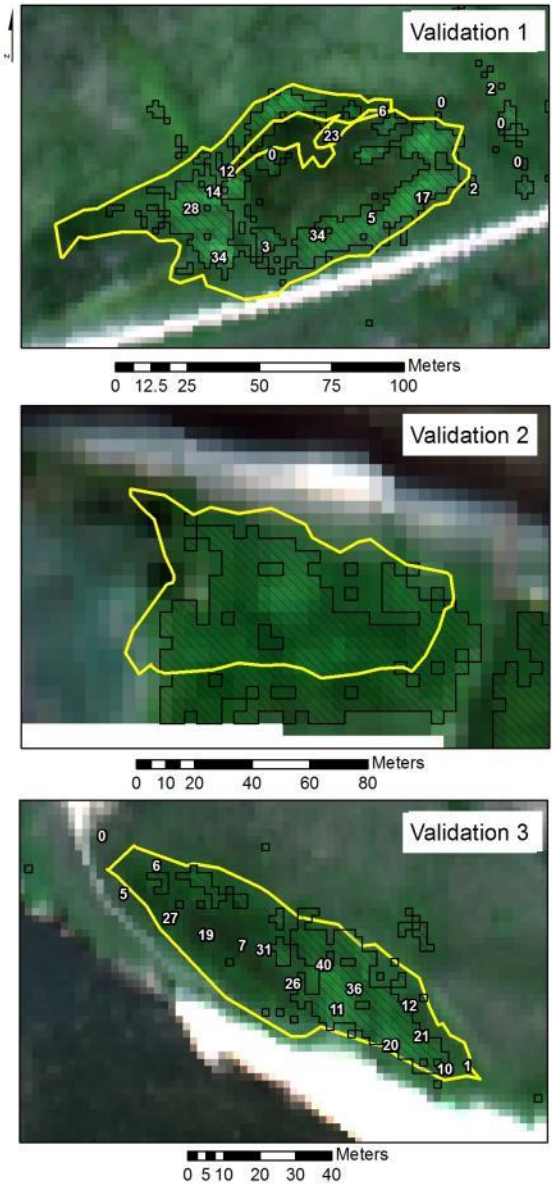

Figure 4-32: Results of the MESMA classification approach using the spectral range of 495 nm - 668 nm at validation sites 1 (top), 2 (middle), and 3 (bottom) with reference stem density counts overlaid on an AISA image (blue: band 24 (459 nm), green: band 64 (548 nm), and red: band 103 (638 nm)). The yellow polygons show the areas ground surveyed in July of 2012.

Figure 4-33: Field photograph showing the presence of yellow flowering leafy spurge stems at validation site 5 as indicated by the red box. (Note: This site was not accessible for collection of stem density or GPS polygons.)

Results show the ability to competently establish a baseline map of high density leafy spurge infestations. The level of map detail is based on the end user's needs and it would be useful for the end user to be involved in developing the process of detecting leafy spurge in order to select best-fit parameters for detection needs. The density levels detected in this study were found to be suitable for biological control purposes as denser patches are needed to sustain the flea beetle populations. Glenn et al. (2005) also found that a minimum of 40 % leafy spurge land cover was needed for reliable repeatable detection of leafy spurge.

Due to the high costs of acquiring airborne hyperspectral data and the coarse resolution (~30 m) of hyperspectral satellite sensors, current and future work is being investigated to determine whether it is the spatial or spectral resolution of the images that is the most important factor in detecting leafy spurge. Table 4-2 contains a summary of the accuracies for all the classifiers using all the spectral subset ranges. The best results were found using the image spectral subset between 495 nm and 668 nm followed by the 409-nm – 794-nm and 408-nm – 2500-nm ranges. The former was able to identify patches with an average about 10 % accuracy in the low-stem density range, 37 % accuracy in the medium-stem density range and about 83 % in the high-density patches between all the classifiers used. All three algorithms produced similar results with respect to detecting known patches of leafy spurge. There was more confusion with green vegetation and trees/shrubs present in the finished maps that included the SWIR wavelengths.

Table 4-2: Stem density validation results using sites 1a, 1b, and 1c.

Classifier	Wavelength (nm)	Stem Densities Correctly Identified (%)		
		Low	Medium	High
SAM	409 - 2500	13.6	45.4	86.7
	409 - 794	0.1	23.44	71.7
	495 - 668	2.2	28.3	84.4
SAM MNF	409 - 2500	8.1	31.6	68.8
	409 - 794	34.1	53.5	81.5
	495 - 668	3.2	29.0	78.6
MTMF	409 - 2500	1.8	12.3	46.8
	409 - 794	5.7	39.4	85.0
	495 - 668	6.0	40.9	85.0
MESMA	409 - 794	1.8	27.5	79.8
	495 - 668	8.9	44.2	79.2

The size of the leafy spurge patches shown at the four test sites indicate that a finer GSD of approximately 2 m would be ideal for locating current infestations, while the spectral detail of hyperspectral images allows for the ability to distinguish distinct spectral areas in the leafy spurge signature. Use of the inflection points seen in the leafy spurge spectral signature could help to determine, which wavelength ranges (bands) may be most suitable for detecting spurge in images.

CHAPTER 5 CONCLUSIONS

The objectives of this thesis were to determine if leafy spurge of differing stem densities could be separated from other native grassland species using differential reflectance derived from AISA airborne hyperspectral data. The airborne imagery in this study shows promise for detecting the presence/absence of leafy spurge.

Analysis of ground photographs collected during field campaigns show potential for estimating leafy spurge stem density and reducing the time required for in-situ fieldwork. The relationship between the flowering leafy spurge stems and the yellow-green pixels on the ground-based photographs should be further tested to see if the relationship holds for additional sites in other test areas or if it was specific to the date, time, and place that the photographs were collected. In the future, it is recommended that the solar elevation angle and the viewing angle of the photographs be taken into consideration to avoid the presence of unwanted shadows in the resulting photographs. Future work in this area could include the use of high-resolution ortho photographs to help establish flowering leafy spurge patch size and density.

Plots of 6 m x 6 m could be established with many spectra being collected within this area and averaged over the entire plot. Theoretically, a 3-pixel by 3-pixel area is required to ensure that at least one 2-m AISA pixel falls within this designated are on the ground. Because of how leafy spurge grows, we tested differently and an image pixel might not fall on patch fully due to errors with the GPS. More samples of the different

scene elements could also be acquired throughout the entire scene with an emphasis on trying to collect pure samples.

The algorithms, SAM, MTMF and SMA, showed that hyperspectral remote sensing could be used to map leafy spurge patches with stem densities greater than 40 m^{-2}. The combination of the SAM classifier and the MNF transform over the 495 nm – 668 nm range performed the best overall in the field and in the validation without over or under estimating the presence of leafy spurge and provided an overall accuracy of 78.6 %. It was also found that a GSD of 2 m was adequate for detecting the presence this kind of of leafy spurge density patches. However as demonstrated, a minimum density threshold level needs to be established for a successful mapping of leafy spurge.

Independent validation data should be collected at the time of the remotely sensed data acquisition due to the nature of plant variation with climate and weather changes. Two years elapsed between the field campaigns for the initial data collection and the validation data collection. The amount of leafy spurge that was present in the areas changed, making it hard to determine the accuracy of the algorithms investigated with respect to map leafy spurge densities.

Another option instead of using the flowering stage is to collect image data in the fall because the stems appear red in colour, which will make them visible in imagery compared to the surrounding dead vegetation. This would allow the ability to track the start of infestations as the yellow flowering stems appear as patches that have already been well established in that area.

Airborne hyperspectral imagery has the advantage of having the ability to obtain a higher spatial resolution over satellite imagery. Current available hyperspectral satellite technology with a GSD of 30 m or higher, would not have worked for the selected study area due to the relative small patches of the infestation. Airborne imagery also has the advantage that data may be collected during important phenological stages of the leafy spurge, while a satellite system is limited by the temporal resolution and may not be able to collect usable data due to cloud cover. However, satellite data tend to be cheaper and more suited to an operational system.

This study addressed the thesis hypothesis, which was to test the ability to separate leafy spurge using its spectral signature from other grassland elements during the flowering phenological stage. It has shown that remote sensing holds promise for identifying and quantifying areas of significantly high density leafy spurge infestations that require management intervention with tactics such as biological control.

REFERENCES

Adams, B. W., Richman, J., Poulin-Klein, L., France, K., Moisey, D., & McNeil, R. L. (2013). Rangeland Plant Communities for the Dry Mixedgrass Natural Subregion of Alberta. Second Approximation.: Rangeland Management Branch, Policy Division, Alberta Environment and Sustainable Resource Development, Lethbridge, Pub. No. T/040.

Alberta Agriculture and Rural Development. (2005). Welcome to the Alberta Soil Information Viewer Retrieved November 15, 2012.

Andrew, M. E., & Ustin, S. L. (2008). The Role of Environmental Context in Mapping Invasive Plants with Hyperspectral Image Data. Remote Sensing of Environment, 112(12), 4301-4317.

Bell Randell, C., & Lym, R. (2006). Introduction. In R. Bourchier, R. Hansen, R. Lym, A. Norton, D. Olson, C. Bell Randall, M. Schwarzlander & L. Skinner (Eds.), Biology and Biological Control of Leafy Spurge (pp. 1-8).

Best, K. F., Bowes, G. G., Thomas, A. G., & Maw, M. G. (1980). The Biology of Canadian Weeds. 39 Euphorbia Esula L. Canadian Journal of Plant Science, 60(2), 651-663.

Boardman, J. W. (1989). Inversion of Imaging Spectrometry Data Using Singular Value Decomposition. Paper presented at the Geoscience and Remote Sensing Symposium, 1989. IGARSS'89. 12th Canadian Symposium on Remote Sensing., 1989 International.

Boardman, J. W., & Kruse, F. A. (2011). Analysis of Imaging Spectrometer Data Using N - Dimensional Geometry and a Mixture-Tuned Matched Filtering Approach. IEEE Transactions on Geoscience and Remote Sensing, 49(11 PART 1), 4138-4152.

Booth, D. T., & Tueller, P. T. (2003). Rangeland Monitoring Using Remote Sensing. Arid Land Research and Management, 17(4), 455-467.

Canadian Food Inspection Agency. (2008). Invasive Alien Plants in Canada - Technical Report Retrieved November 13, 2012.

Carson, H. W., Lass, L. W., & Callihan, R. H. (1995). Detection of Yellow Hawkweed (Hieracium Pratense) with High Resolution Multispectral Digital Imagery. Weed Technology, 9(3), 477-483.

Casady, G. M., Hanley, R. S., & Seelan, S. K. (2005). Detection of Leafy Spurge (Euphorbia Esula) Using Multidate High-Resolution Satellite Imagery. Weed Technology, 19(2), 462-467.

Colautti, R. I., Bailey, S. A., Van Overdijk, C. D. A., Amundsen, K., & MacIsaac, H. J. (2006). Characterised and Projected Costs of Nonindigenous Species in Canada. Biological Invasions, 8(1), 45-59.

Defries, R. S., & Townshend, J. R. G. (1999). Global Land Cover Characterization from Satellite Data: From Research to Operational Implementation? Global Ecology and Biogeography, 8(5), 367-379.

DiTomaso, Joseph M. (2000). Invasive Weeds in Rangelands: Species, Impacts, and Management. Weed Science, 48(2), 255-265.

Elmore, A. J., Mustard, J. F., Manning, S. J., & Lobell, D. B. (2000). Quantifying Vegetation Change in Semiarid Environments: Precision and Accuracy of Spectral Mixture Analysis and the Normalized Difference Vegetation Index. Remote Sensing of Environment, 73(1), 87-102.

Environment Canada. (2012). Daily Data Report for July 2010. Retrieved November 15, 2012.

Everitt, James H., Anderson, Gerald L., Escobar, David E., Davis, Michael R., Spencer, Neal R., & Andrascik, Roger J. (1995a). Use of Remote Sensing for Detecting and Mapping Leafy Spurge (Euphorbia Esula). Weed Technology, 9(3), 599-609.

Everitt, James H., Escobar, David E., & Davis, Michael R. (1995b). Using Remote Sensing for Detecting and Mapping Noxious Plants. Weed Abstracts (United Kingdom).

Foody, G. M., Campbell, N. A., Trodd, N. M., & Wood, T. F. (1992). Derivation and Applications of Probabilistic Measures of Class Membership from the Maximum-Likelihood Classification. Photogrammetric Engineering & Remote Sensing, 58(9), 1335-1341.

Gauthier, D. A., & Wiken, E. D. B. (2003). Monitoring the Conservation of Grassland Habitats, Prairie Ecozone, Canada. Environmental Monitoring and Assessment, 88(1-3), 343-364.

Glenn, N. F., Mundt, J. T., Weber, K. T., Prather, T. S., Lass, L. W., & Pettingill, J. (2005). Hyperspectral Data Processing for Repeat Detection of Small Infestations of Leafy Spurge. Remote Sensing of Environment, 95(3), 399-412.

Goodenough, D. G., Niemann, K. O., Dyk, A., Hobart, G., Gordon, P., Loisel, M., & Chen, H. (2008). Comparison of Aviris and Aisa Airborne Hyperspectral Sensing for above-Ground Forest Carbon Mapping.

Goodenough, D. G., Niemann, K. O., Quinn, G. S., Gordon, P., Gross, A., Han, T., Hobart, G., Chen, H., & Dyk, A. (2009). Comparison of Aviris and Aisa for Chemistry Mapping.

Green, A. A., Berman, M., Switzer, P., & Craig, M. D. (1988). A Transformation for Ordering Multispectral Data in Terms of Image Quality with Implications for Noise Removal. IEEE Transactions on Geoscience and Remote Sensing, 26(1), 65-74.

Haboudane, D., Miller, J. R., Pattey, E., Zarco-Tejada, P. J., & Strachan, I. B. (2004). Hyperspectral Vegetation Indices and Novel Algorithms for Predicting Green Lai of Crop Canopies: Modeling and Validation in the Context of Precision Agriculture. Remote Sensing of Environment, 90(3), 337-352.

Hansen, R. W., Richard, R. D., Parker, P. E., & Wendel, L. E. (1997). Distribution of Biological Control Agents of Leafy Spurge (Euphorbia Esula L.) in the United States: 1988-1996. Biological Control, 10(2), 129-142.

Harsanyi, J. C., Chang, C. I., & Johns Hopkins, Univ. (1993). Hyperspectral Image Dimensionality Reduction and Pixel Classification - an Orthogonal Subspace Projection Approach. Proceedings of the Twenty-Seventh Annual Conference on Information Sciences and Systems, 401-406.

Hein, David G., & Miller, Stephen D. (1992). Influence of Leafy Spurge on Forage Utilization by Cattle. Journal of Range Management, 45(4), 405-407.

Hodur, N. M., Leistritz, F. L., & Bangsund, D. A. (2006). Biological Control of Leafy Spurge: Utilization and Implementation. Rangeland Ecology and Management, 59(5), 445-452.

Hunt, E. Raymond, Daughtry, C. S. T., Kim, M. S., & Williams, A. E. P. (2007). Using Canopy Reflectance Models and Spectral Angles to Assess Potential of Remote Sensing to Detect Invasive Weeds. Journal of Applied Remote Sensing, 1(1).

Jensen, J.R. (2005). Introductory Digital Image Processing: A Remote Sensing Perspective: Prentice Hall.

Johannsen, C. J., & Barney, T. W. (1981). Remote Sensing Applications for Resource Management. Journal of Soil & Water Conservation, 36(3), 128-133.

Kerr, J.T., & Ostrovsky, M. (2003). From Space to Species: Ecological Applications for Remote Sensing. Trends in Ecology & Evolution, 18(6), 299-305.

Knipling, E.B. (1970). Physical and Physiological Basis for the Reflectance of Visible and near-Infrared Radiation from Vegetation. Remote Sensing of Environment, 1(3), 155-159.

Kruse, F. A., Lefkoff, A. B., Boardman, J. W., Heidebrecht, K. B., Shapiro, A. T., Barloon, P. J., & Goetz, A. F. H. (1993). The Spectral Image Processing System (Sips)—Interactive Visualization and Analysis of Imaging Spectrometer Data. Remote Sensing of Environment, 44(2–3), 145-163.

Lass, L.W., & Callihan, R.H. (1997). The Effect of Phenological Stage on Detectability of Yellow Hawkweed (Hieracium Pratense) and Oxeye Daisy (Chrysanthemum Leucanthemum) with Remote Multispectral Digital Imagery. Weed Technology, 248-256.

Lass, L.W., Carson, H.W., & Callihan, R.H. (1996). Detection of Yellow Starthistle (Centaurea Solstitialis) and Common St. Johnswort (Hypericum Perforatum) with Multispectral Digital Imagery. Weed Technology, 10(3), 466-474.

Lass, L.W., Thill, D.C., Shafii, B., & Prather, T.S. (2002). Detecting Spotted Knapweed (Centaurea Maculosa) with Hyperspectral Remote Sensing Technology. Weed Technology, 16(2), 426-432.

Leafy Spurge Stakeholders Group. (1999). Leafy Spurge Economic Impact Assessment. Brandon University, Brandon, MB: WESTARCH Group Inc.

Lee, J. B., Woodyatt, S., & Berman, M. (1990). Enhancement of High Spectral Resolution Remote-Sensing Data by a Noise-Adjusted Principal Components Transform. [Article]. IEEE Transactions on Geoscience and Remote Sensing, 28(3), 295-304.

Lu, G.Y., & Wong, D.W. (2008). An Adaptive Inverse-Distance Weighting Spatial Interpolation Technique. Computers & Geosciences, 34(9), 1044-1055.

Luciuk, G. M., Bristol, B., Weins, T. W., & Boyle, D. M. (1997). The Potential Impact of Endangered Species Legislation on Federal Grazing Lands and the Livestock Industry. Paper presented at the Proceedings of XVIII International Grassland Congress, Winnipeg, MB.

Marsett, R. C., Qi, J., Heilman, P., Biedenbender, S. H., Watson, M. C., Amer, S., Weltz, M., Goodrich, D., & Marsett, R. (2006). Remote Sensing for Grassland Management in the Arid Southwest. Rangeland Ecology and Management, 59(5), 530-540.

Masters, R.A, & Sheley, R.L. (2001). Principles and Practices for Managing Rangeland Invasive Plants. Journal of Range Management, 54(5), 502-517.

McCloud, P. I., & Darroch, J. N. (1995). An Analysis of Categorical Repeated Measurements in the Presence of an External Factor. Biometrika, 82(1), 47-55.

Mitchell, J.J., & Glenn, N.F. (2009). Leafy Spurge (Euphorbia Esula) Classification Performance Using Hyperspectral and Multispectral Sensors. Rangeland Ecology & Management, 62(1), 16-27.

Mladinich, C. S., Bustos, M. R., Stitt, S., Root, R., Brown, K., Anderson, G. L., & Hager, S. (2006). The Use of Landsat 7 Enhanced Thematic Mapper Plus for Mapping Leafy Spurge. Rangeland Ecology and Management, 59(5), 500-506.

Natural Regions Committee. (2006). Natural Regions and Subregions of Alberta. In D. J. Downing & W. W. Pettapiece (Eds.): Government of Alberta, Pub. No. T/852.

Noujdina, N.V., & Ustin, S.L. (2009). Mapping Downy Brome (Bromus Tectorum) Using Multidate Aviris Data. Weed Science, 56(1), 173-179.

O'Neill, M., Ustin, S.L., Hager, S., & Root, R. (2000). Mapping the Distribution of Leafy Spurge at Theodore Roosevelt National Park Using AVIRIS. *In*: Green, R. O., editor. *Proceedings of the 9th JPL Airborne Earth Science Workshop*. Pasadena, CA, USA NASA Jet Propulsion Laboratory Publication. 1.

Otterman, J., Lowman, P. D., & Salomonson, V. V. (1976). Surveying Earth Resources by Remote Sensing from Satellites. Geophysical Surveys, 2(4), 431-467.

Parker Williams, A., & Hunt, E. R.. (2002). Estimation of Leafy Spurge Cover from Hyperspectral Imagery Using Mixture Tuned Matched Filtering. Remote Sensing of Environment, 82(2-3), 446-456.

Parker Williams, A., & Hunt, E. R. (2004). Accuracy Assessment for Detection of Leafy Spurge with Hyperspectral Imagery. Journal of Range Management, 57(1), 106-112.

Peddle, D.R., White, H.P., Soffer, R.J., Miller, J.R., & LeDrew, E.F. (2001). Reflectance Processing of Remote Sensing Spectroradiometer Data. Computers & Geosciences, 27(2), 203-213.

Powell, R.L., Roberts, D.A., Dennison, P.E., & Hess, L.L. (2007). Sub-Pixel Mapping of Urban Land Cover Using Multiple Endmember Spectral Mixture Analysis: Manaus, Brazil. Remote Sensing of Environment, 106(2), 253-267.

Purkis, S.J., & Klemas, V.V. (2011). Remote Sensing and Global Environmental Change. Wiley-Blackwell. Chichester, U.K.

Richardson, A. J., & Wiegand, A. L. (1977). Distinguishing Vegetation from Soil Background Information. Photogrammetric Engineering and Remote Sensing, 43(12), 1541-1552.

Richter, R., & Schlapfer, D. (2002). Geo-Atmospheric Processing of Airborne Imaging Spectrometry Data. Part 2: Atmospheric/Topographic Correction. International Journal of Remote Sensing, 23(13), 2631-2649.

Roberts, E. A., Sheley, R. L., & Lawrence, R. L. (2004). Using Sampling and Inverse Distance Weighted Modeling for Mapping Invasive Plants. Western North American Naturalist, 64(3), 312-323.

Sabin, Michael J. (1987). Convergence and Consistency of Fuzzy C-Means/Isodata Algorithms. Pattern Analysis and Machine Intelligence, IEEE Transactions on, PAMI-9(5), 661-668.

Schläpfer, D., Borel, C.C., Keller, J., & Itten, K.I. (1998). Atmospheric Precorrected Differential Absorption Technique to Retrieve Columnar Water Vapor. Remote Sensing of Environment, 65(3), 353-366.

Singh, A., & Harrison, A. (1985). Standardized Principal Components. International Journal of Remote Sensing, 6(6), 883-896.

Singh, N., & Glenn, N. F. (2009). Multitemporal Spectral Analysis for Cheatgrass (Bromus Tectorum) Classification. International Journal of Remote Sensing, 30(13), 3441-3462.

Smith, A.M., & Buckley, J.R. (2011). Investigating Radarsat-2 as a Tool for Monitoring Grassland in Western Canada. Canadian Journal of Remote Sensing, 37(1), 93-102.

Stitt, S., Root, R., Brown, K., Hager, S., Mladinich, C., Anderson, G. L., Dudek, K., Bustos, M. R., & Kokaly, R. (2006). Classification of Leafy Spurge with Earth Observing-1 Advanced Land Imager. Rangeland Ecology and Management, 59(5), 507-511.

Tueller, P.T. (1989). Remote Sensing Technology for Rangeland Management Applications. Journal of Range Management, 42(6), 442-453.

Turner II, B. L., & Meyer, W.B. (1991). Land Use and Land Cover in Global Environmental Change: Considerations for Study. [Article]. International Social Science Journal, 43(4), 669.

Ustin, S. L., & Gamon, J. A. (2010). Remote Sensing of Plant Functional Types. New Phytologist, 186(4), 795-816.